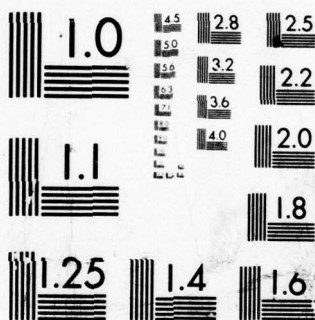MICROCOPY RESOLUTION TEST CHART

NATIONAL BUREAU OF STANDARDS-1963-A

LEVEL

②
NW

NAVAL POSTGRADUATE SCHOOL
Monterey, California

Master's THESIS

The Effects of a Prescribed Salinity
Field on a 10-Level Primitive Equation
Ocean Circulation Model

by

Kenneth Eicher Barbor

72p.

Dec   78

Thesis Advisor: R. L. Haney

251 450

79 03 26 027

REPORT DOCUMENTATION PAGE		READ INSTRUCTIONS BEFORE COMPLETING FORM
1. REPORT NUMBER	2. GOVT ACCESSION NO.	3. RECIPIENT'S CATALOG NUMBER
4. TITLE (and Subtitle) The Effects of a Prescribed Salinity Field on a 10-Level Primitive Equation Ocean Circulation Model		5. TYPE OF REPORT & PERIOD COVERED Master's Thesis; December 1978
		6. PERFORMING ORG. REPORT NUMBER
7. AUTHOR(s) Kenneth Eicher Barbor		8. CONTRACT OR GRANT NUMBER(s)
9. PERFORMING ORGANIZATION NAME AND ADDRESS Naval Postgraduate School Monterey, California 93940		10. PROGRAM ELEMENT, PROJECT, TASK AREA & WORK UNIT NUMBERS
11. CONTROLLING OFFICE NAME AND ADDRESS Naval Postgraduate School Monterey, California 93940		12. REPORT DATE December 1978
		13. NUMBER OF PAGES 71
14. MONITORING AGENCY NAME & ADDRESS(If different from Controlling Office)		15. SECURITY CLASS. (of this report) Unclassified
		15a. DECLASSIFICATION/DOWNGRADING SCHEDULE

16. DISTRIBUTION STATEMENT (of this Report)

Approved for public release; distribution unlimited.

17. DISTRIBUTION STATEMENT (of the abstract entered in Block 20, if different from Report)

18. SUPPLEMENTARY NOTES

19. KEY WORDS (Continue on reverse side if necessary and identify by block number)

20. ABSTRACT (Continue on reverse side if necessary and identify by block number)

A prescribed salinity field is inserted into a 10-level primitive equation ocean circulation model. The model has been developed and is being improved in order to study large-scale thermal anomalies observed in the Central North Pacific Ocean by the North Pacific Experiment (NOR-PAX). The salinity field, based on observations along 160 W longitude, is independent of longitude and time, and is smoothed in the north-south direction to remove small-scale variations. A new equation of state CONT'

DD FORM 1473 EDITION OF 1 NOV 65 IS OBSOLETE
1 JAN 73
(Page 1)   S/N 0102-014-6601 |

CONT'

which is a function of temperature, salinity and depth is used to determine density in the calculation of pressure from the hydrostatic equation. The parameterization of vertical mixing is changed to account for the stabilizing effect of salinity and the supercooling of the surface layers at high latitudes during winter.

The addition of salinity induced changes in the currents at high latitudes when compared to the model without salinity. A Rossby wave was excited in the middle latitudes which produced transient changes. The convective adjustment process enabled significantly colder water to overlie warmer water in the regions where salinity increases with depth. Supercooled surface temperatures, encountered during winter at high latitudes, are handled through convective mixing, but further investigation into the dynamics of sub-grid scale vertical convection at near freezing temperatures is recommended.

ACCESSION for

NTIS   White Section
DDC   B H Section   ☐
                                         ☐
J.S.

BY
DISTRIBUTION/AVAILABILITY CODES
Dist.   SPECIAL

A

79 03 26 077

The Effects of a Prescribed Salinity
Field on a 10-Level Primitive Equation
Ocean Circulation Model

by

Kenneth Eicher Barbor
Lieutenant, United States Navy
B.S., University of Michigan, 1972

Submitted in partial fulfillment of the
requirements for the degree of

MASTER OF SCIENCE IN METEOROLOGY AND OCEANOGRAPHY

from the

NAVAL POSTGRADUATE SCHOOL
December 1978

Author _____

Approved by: _____
                                        Thesis Advisor

_____
                                        Second Reader

_____
                Chairman, Department of Meteorology

_____
                Dean of Science and Engineering

3

ABSTRACT

A prescribed salinity field is inserted into a 10-level primitive equation ocean circulation model. The model has been developed and is being improved in order to study large-scale thermal anomalies observed in the Central North Pacific Ocean by the North Pacific Experiment (NOR-PAX). The salinity field, based on observations along 160 W longitude, is independent of longitude and time, and is smoothed in the north-south direction to remove small-scale variations. A new equation of state which is a function of temperature, salinity and depth is used to determine density in the calculation of pressure from the hydrostatic equation. The parameterization of vertical mixing is changed to account for the stabilizing effect of salinity and the supercooling of the surface layers at high latitudes during winter.

The addition of salinity induced changes in the currents at high latitudes when compared to the model without salinity. A Rossby wave was excited in the middle latitudes which produced transient changes. The convective adjustment process enabled significantly colder water to overlie warmer water in the regions where salinity increases with depth. Supercooled surface temperatures, encountered during winter at high latitudes, are handled through convective mixing, but further investigation into the dynamics of sub-grid scale vertical convection at near freezing temperatures is recommended.

TABLE OF CONTENTS

LIST OF TABLES

LIST OF FIGURES

ACKNOWLEDGEMENTS

The author wishes to express his appreciation to Dr. Robert L. Haney for his guidance, understanding and counsel in the preparation of this thesis and to Dr. G. H. Jung for reading the thesis and making useful comments.

Special appreciation is given to my loving wife whose understanding and patience enabled me to complete the necessary research.

I. INTRODUCTION

The ocean and atmosphere behave as a coupled system with anomalies
in one medium inducing anomalies in the other. Bjerknes (1966, 1969,
1972) and Namias (1959, 1969, 1972) have investigated this interaction by
relating observed sea-surface temperature (SST) anomalies to anomalous
behavior in the atmosphere. Other investigations have been conducted
with numerical simulations to test the response of the atmosphere to a
prescribed ocean (Rowntree, 1972), the response of the ocean to a pre-
scribed atmosphere (Haney, 1974) or the simultaneous effects of a coupled
system (Manabe, 1969; Bryan, 1969; Wetherald and Manabe, 1972). Through
observations and numerical simulations a greater understanding of the
air-sea system is sought with improved forecasting of the atmospheric and
oceanic variability an ultimate goal.

The numerical model used in this investigation is that of Haney (1974)
with subsequent improvements involving seasonal atmospheric forcing, para-
meterization of convective mixing and surface wind stirring (Haney and
Davies, 1976) and nonlinear eddy viscosity (Haney and Wright, 1975). The
goal of this investigation is to further improve this model by introducing
salinity as a new variable. The model, based on the hydrostatic and
Boussinesq approximation, is a 10-level primitive equation model in a
closed rectangular basin with uniform depth of 4 kilometers. The basin
which extends from the equator to 65°N and spans 90° of longitude is an
idealized representation of the North Pacific Ocean. The horizontal re-
solution of approximately 2° of latitude and 3° of longitude is provided
by 33 uniformly spaced grid points in the north-south and east-west

directions. In the vertical, the ten levels are located at 10, 32.5, 62.5, 102.5, 162.5, 462.5, 900, 1700 and 3100 meters below the surface. Wind and differential heating which drive the ocean circulation are derived from prescribed but time varying climatological values of solar radiation, cloudiness, surface air temperature, surface specific humidity and winds. Until the present study, the density in the model was assumed to be a linear function of temperature only.

The model has been developed and is being improved in order to study large-scale thermal anomalies observed in the Central North Pacific Ocean by the North Pacific Experiment (NORPAX).

During a "spin-up" phase, the model is integrated for approximately 240 years of simulated time to produce a "model climatology". The resulting circulation and temperature patterns adequately represent the large-scale north-south temperature variations and the major ocean gyres; however, the Alaskan gyre is not depicted. Once the model climatology has been established, temperature anomalies are injected into the model which is then integrated forward in time with or without anomalous atmospheric forcing. The evolution and migration of these anomalies can be related to their horizontal or vertical extent and atmospheric conditions to determine the controlling processes. Investigations by Hunt (1975) and Shiver (1977) detail the use of this model in such studies of large-scale ocean variability and the major conclusions of these works are published in Haney, Shiver and Hunt (1978).

The motivation for this investigation is to determine the effects of adding a prescribed salinity cross section to the model. The salinity cross section is steady state and independent of longitude. This new salinity field modifies the density field through a newly introduced

11

equation of state. The resulting modifications to the density field affect the hydrostatic pressure, and hence the horizontal pressure gradient, as well as the vertical stability.

This introduction of a prescribed salinity cross section is expected to improve the model in several ways. First, as noted above, the present model climatology (without salinity) does not depict an Alaskan gyre. Part of this model's deficiency may be due to the somewhat idealized form of the wind forcing at high latitudes; however, temperature variations are small and salinity can play an important role in the density structure and hence, the geostrophic flow. Thus it is expected that salinity may improve the model's circulation at high latitudes. The desirability of adequately simulating the Alaskan gyre in this meteorologically significant area is apparent.

In his work using the model in which density depended on temperature only, Hunt (1975) noted that cold SST anomalies could not be maintained in the winter at high latitudes but were immediately convectively mixed downward. Cold SST anomalies are a physically realizable condition during winter in high latitudes. Surface cooling occurs but the increasing salinity with depth provides stability and maintains the cold surface anomaly. However, free convection occurs and must be modeled whenever the surface layers become more dense than the underlying layers. The model previously determined stability solely from the temperature profile. If the temperature decreases with depth (positive profile), the profile is stable and convection does not occur. On the other hand, an unstable profile (produced for example by a cold surface anomaly) is instantaneously adjusted to neutral thereby destroying any cold surface anomalies which produced the instability. In reality, density, and therefore

12

stability, is a complex function of temperature, salinity and depth and
a negative temperature profile can be stabilized by a positive salinity
profile. In this manner, cold SST anomalies can be formed and maintained
and one of the goals of this study is to make the model more realistic
in this regard. Similarly, but with less apparent significance, a warm
anomaly can be maintained below the surface layers. The inclusion of
salinity in the model can play an important role in the study of large-
scale thermal anomalies by improving the climatological circulation pat-
tern and altering the vertical stability, and hence, the convective
adjustment parameterization.

II. DATA COMPILATION AND HANDLING

The salinity cross section used in the model is steady state and in-
dependent of longitude. The steady state assumption was necessitated
by the lack of data. A seasonal variation in surface salinity tied to
the variation in evaporation is known to exist in several geographical
areas. Other temporal variations in surface salinity exist at high lati-
tudes where ice formation or melting alters the salinity profile. How-
ever, the extent, both vertically and horizontally, to which these
variations influence the open ocean are not known and can not be ade-
quately modeled (Sverdrup et al., 1942).

Allowing salinity to vary only latitudinally was dictated primarily
by simplicity and economy; however, the dependence in Y alone is justi-
fiable. The significant gradients in salinity are north-south and ap-
preciable deviations from this pattern are found only at the boundaries
where land runoff and boundary currents become important (Figure 1)
(Riley and Skirrow, 1975). Since the model is primarily concerned with
open ocean circulation, the assumption of longitudinal independence in
salinity seems reasonable. An anticipated result of the inclusion of
salinity into the model is the formation of an improved and more realis-
tic subarctic gyre. This gyre could be created by the geostrophic flow
induced by a north-south salinity gradient.

The salinity cross section prescribed in the model was derived from
actual measurements from research vessels. The series, Oceanic Observa-
tions of the Pacific: (Year) (Scripps Institution, 1960; 1963a and b;

14

1965a,b,c and d) compiled by Scripps Institution of Oceanography was the source of the measurements. Salinity profiles were selected to approximate a cross section along 160°W longitude and at the model's grid point spacing of 2.03° latitude. Due to the sparseness of data in some areas, a common time of year could not be selected; however, 75% of the measurements lie between late spring and early fall. Because the Pacific Ocean narrows and shoals above 60°N, data in this area are limited in both horizontal and vertical extent. To overcome the data insufficiencies the profile at 60°N was duplicated for the grid points between 60°N and the model's boundary which is located at 65°N.

Figure 2 shows the latitude-height cross section, taken from the above data sources, plotted and analyzed at the model's grid points. The salinity cross section (Figure 3) found in <u>Intermediate Waters of the Pacific Ocean</u> (Reid, 1965) was used to verify the representativeness of the compiled cross section. Major features such as the low salinity tongue penetrating equatorward from the high latitudes and the high salinity central water mass are adequately represented. Areas of sharp horizontal gradients at 35°N and 45°N are also reasonably depicted.

Although the major features of the salinity cross section were well represented, a smoothing technique was employed to remove the small-scale irregularities and improve horizontal consistency. A repeated, three point weighted average given by

$$S_{j,k}^* = .25\ S_{j-1,k} + .5\ S_{j,k} + .25\ S_{j+1,k} \tag{1}$$

was selected. Boundary values remained unchanged. This smoothing process was performed up to five times and the resulting cross sections analyzed. Four repetitions of this averaging scheme removed small-scale

15

irregularities (less than two grid lengths) but retained the major features of the salinity structure (Figure 4). The central water mass remains intact and the low salinity tongue is still identifiable. Horizontal gradients have been smoothed but maintain their location and a portion of their intensity. Since the cross section was composed of actual soundings, vertical consistency was assured and vertical smoothing was not considered necessary.

III.   EQUATION OF STATE AND CONVECTIVE ADJUSTMENT

The density of sea water as a function of temperature, salinity and pressure is usually computed using the Knudsen formula. Although the Knudsen formula is quite accurate, it is generally considered too inefficient for inclusion in numerical models. This inefficiency arises due to the wide range of temperature and salinity for which the Knudsen formula holds. Since the actual variation of temperature and salinity in the open ocean is known to be limited, several researchers have developed empirical formulas which are accurate and efficient but apply only to open ocean temperature and salinity ranges. Two such empirical formulas were considered for inclusion in the model.

Bryan and Cox (1972) solved an overdetermined, simultaneous system of equations which related departures from the mean of temperature and salinity to the departure from the mean density at a given depth. That is:

$$
\begin{bmatrix} \delta T_1 & \delta S_1 & \delta T_1^2 & \delta S_1^2 & \delta T_1 S_1 & \cdots \\ \delta T_2 & \delta S_2 & \cdots & & & \\ \vdots & \vdots & & & & \\ \delta T_m & \delta S_m & \cdots & & & \end{bmatrix}
\begin{bmatrix} x_{1k} \\ x_{2k} \\ \vdots \\ x_{nk} \end{bmatrix}
=
\begin{bmatrix} \rho_1 - \rho_{0k} \\ \rho_2 - \rho_{0k} \\ \vdots \\ \rho_m - \rho_{0k} \end{bmatrix} \quad m > n
\tag{2}
$$

where: $\delta T_k = (T_k - T_{0k})$

$\delta S_k = (S_k - S_{0k})$

T_{0k}, ρ_{0k} and S_{0k} are the mean values at a given depth.

The density is given by:

$$x_{1k}\delta T + x_{2k}\delta S + x_{3k}(\delta T)^2 + x_{4k}(\delta S)^2 + x_{5k}\delta T\delta S = [\rho(T,S,Z_k)-\rho_{0k}]\times 10^3$$

(3)

The constant coefficients, x_n, were computed at each depth by Bryan and Cox using an iterative process. Acceptable accuracy was obtained with as few as three coefficients (n=3) and 50 temperature, salinity and density combinations (m=50). A significant improvement in accuracy was obtained with nine coefficients (n=9, m=50). Figure 5 illustrates the accuracy of this method as compared to the Knudsen formula. The errors are always largest near the surface where the widest range of temperatures and salinities exist.

Another empirical formula for the equation of state of sea water was developed by Friedrich and Levitus (1972). This formula is similar to the Bryan and Cox formula in that it fits a polynomial in temperature and salinity to computed values of density determined by the Knudsen formula; however, the coefficients are continuous, rather than discrete, functions of depth.

A quadratic equation given by

$$\sigma(T,S,Z) = C_1 + C_2T + C_3S + C_4T^2 + C_5TS$$

(4)

is highly efficient but is not sufficiently accurate over the expected range of temperature and salinity. Further expansion of the polynomial to

$$\sigma(S,T,Z) = C_1 + C_2T + C_3S + C_4T^2 + C_5ST + C_6T^3 + C_7ST^2$$

(5)

18

yields acceptable accuracy while expansion to more terms does not improve accuracy appreciably.

The coefficients are themselves quadratic polynomials in -Z (depth) which fit a smoothed curve to the pressure dependency of density. Due to the reduced range of temperature and salinity with depth, the coefficients more accurately represent the pressure dependence at increased depth. Figure 6 shows the pressure dependence of the coefficients and the rms error of equation (5) with respect to the Knudsen formula. Increased efficiency without a decrease in accuracy can be accomplished by reverting to equation (4) at depths of two kilometers and below. The values for the coefficients used in equations (4) and (5) are given in Tables I and II, respectively. Note that Z is in kilometers and defined positive downward.

The Friedrich and Levitus equation of state was selected for inclusion in the model since computation of density at the model's irregular depths is facilitated by the continuous depth dependence. Another advantage over equation (3) of this formulation is that the equation of state would not have to be changed if the location of the levels in the model were ever changed. The explicit depth, temperature and salinity dependence of density as set forth by equation (5) aids in the remodeling of the convective adjustment process as discussed below.

Without salinity the model had convectively adjusted whenever the profile was slightly positive, neutral or negative. The incorporation of salinity into the model enables a negative temperature profile to be convectively stable when coupled with a stabilizing salinity profile. To determine the relationship between depth, temperature, salinity and density, the total derivative was expanded into its components.

19

$$\frac{d\sigma}{dZ} = \frac{\partial\sigma}{\partial Z} + \frac{\partial\sigma}{\partial T}\frac{\partial T}{\partial Z} + \frac{\partial\sigma}{\partial S}\frac{\partial S}{\partial Z} , \qquad (6)$$

where Z increases upward. For stability, $\frac{d\sigma}{dZ} \leq 0$, the temperature profile must satisfy

$$\frac{\partial T}{\partial Z} \geq (- \frac{\partial\sigma}{\partial Z} - \frac{\partial\sigma}{\partial S}\frac{\partial S}{\partial Z}) / \frac{\partial\sigma}{\partial T} . \qquad (7)$$

$$(1) \qquad (2) \quad (3) \quad (4) \quad (5)$$

The right hand side of equation (7) gives the temperature lapse rate which renders the density profile neutral ($\frac{d\sigma}{dZ} = 0$). Terms (1) and (4) are known from the temperature and salinity profiles computed in the model. Terms (2), (3) and (5) are computed from the equation of state [equation (5)]. For efficiency, terms (2) and (3) can be simplified through scale analysis; however, all components of term (5) can be of similar magnitude and must therefore be retained. The expansion of the terms in equation (7) and the scale analysis is detailed in Appendix A. If the inequality is violated (as calculated using finite differencing between two levels), then the temperature profile is convectively adjusted. The adjustment is accomplished by satisfying two constraints:

1) the heat present in the two layers remains constant; and

2) the new temperature profile equals the neutral temperature lapse rate, the right hand side of equation (7), plus a small additional stabilizing lapse rate.

In this manner, cold water may overlie warm water provided the proper salinity structure exists.

20

IV. RESULTS

A "spin up" of 246 years of simulated time without salinity (Haney et al., 1978) was used as initial conditions. The salinity cross section and equation of state discussed above were inserted into the model and the integration continued for seven years. Streamlines and temperature contours at various depths for summer (mid-July) and winter (mid-January) of the model climatology, year 246 (without salinity) and the years 249 through 253 (with salinity) were plotted, analyzed and compared. During the first seven year integration period, "neutral stability" was still defined as $\frac{\partial T}{\partial Z} = 0$. That is, the stabilizing effect of salinity in the parameterization of vertical convection (convective adjustment) was not included. This effect was added after year 253 (see below). It was handled in this manner in order to study the effects of one change at a time. The model climatology, without salinity, Figures 7 through 11, depict the features previously discussed. In these and subsequent stream-line figures, the lengths of the small arrows are indicative of the rela-tive magnitude of the current at the grid point, while the long continuous lines are streamlines which help display the flow direction. In both the winter and summer the Equatorial Counter Current, North Equatorial Cur-rent, Kuroshio Current and North Pacific Current are well represented. At high latitudes a cyclonic turning is apparent but a closed Alaskan gyre is not formed. The temperature contours, Figures 12 through 16, illustrate the baroclinic zone formed by the North Pacific Current and the northward displacement of this baroclinic zone by the Kuroshio Current. The contour interval is 3°C at all levels except at level 9 where the

21

interval is 0.3°C. The North Pacific Central Water Mass is well defined in horizontal and vertical extent by the 21°C isotherm.

After seven years of integration with salinity included, several changes in the streamline and temperature contours are visible. Comparing Figures 17 through 26 to their counterparts in the model climatology reveals a lessening of the cyclonic tendencies of the surface layers at high latitudes in the model with salinity included. Since this is directly opposed to the anticipated results, it merits further investigation.

In the previous model with the equation of state represented by a linear function of temperature, the north-south gradients of temperature near 0°C, although small, generated significant geostrophic currents. Wind generated currents provided the cyclonic tendencies in the surface layers. The present equation of state is only weakly affected by the temperature fluctuations at low temperatures. The salinity gradients at high latitudes are very weak (recall, there is no horizontal salinity gradient from 60°N to 65°N) with the resulting current primarily induced by the wind fields (Figure 27). A strongly zonal forcing during winter generates meridional surface currents at high latitudes with the converse applying during summer. Below the surface, zonal currents resulting from the north-south temperature and salinity gradients are encountered but their magnitudes are small.

Another feature of interest, which appears during winter (Figures 17a through 21a) when salinity is included, is the southward directed current along the western boundary near 45°N. This current is physically located in the region of the Oyashio Current. It appears only in winter, and since salinity is constant all year, atmospheric forcing is the

22

logical cause. The transport stream function (the vertically integrated mass transport is nondivergent and therefore represented by a stream function in this "rigid lid" model) for winter as compared to summer (Figure 28) explains the seasonal dependence of this gyre. A strong cyclonic stream function is located in this region in the winter while the value of the stream function in this area is small during summer. The salinity cross section (Figure 4) below 125 meters enhances the cyclonic shear due to a local salinity maximum coincident with the axis of the stream function minimum. The resulting streamlines depict a geostrophic gyre below 100 meters and a wind induced gyre above 100 meters. When the cyclonic atmospheric forcing diminishes in the summer, the upper levels revert to a zonal flow and the gyre disappears except at the lower levels.

A third change noted with the inclusion of salinity is a rather large cyclonic vortex in the eastern portion of the domain at about 35°N. A time series of streamlines from July 248 through July 251 (Figures 29 through 32) show that the vortex is propagating westward at a rate of approximately 1.6 cm/sec. The vortex is present both winter and summer and penetrates from the surface to approximately 350 meters. The characteristics of this vortex point to an internal Rossby wave. The phase speed of an internal Rossby wave is given by

$$c = U - \frac{\beta}{1^2 + k^2 + \frac{m^2 f_o^2}{N^2}} \tag{8}$$

where U = speed of the mean current

1, k and m are the wave numbers in the x, y and z directions and $1 = 2\pi/L$

f_o = average value for the Coriolis parameter

β = change in f with latitude

$N = (\alpha g \frac{\partial T}{\partial Z})^{\frac{1}{2}}$ the Brunt-Vaisala frequency

This equation is based on a constant mean flow, U, and a Brunt-Vaisala frequency, N, which is qualitatively applicable to the region in question. Values for the above equation were determined from the streamline plots, temperature profiles and velocity fields. The following values were selected:

$$f_o = 2\Omega \sin\phi = 2\Omega \sin 35.5 = 8.4 \times 10^{-5} \text{ sec}^{-1}$$

$$\beta = \frac{f_{36} - f_{35}}{111 \times 10^5 \text{ cm}} = 1.9 \times 10^{-13} \text{ sec}^{-1} \text{ cm}^{-1}$$

$$l = 2\pi/1000 \text{ km}$$

$$k = 2\pi/3000 \text{ km}$$

$$m = 2\pi/800 \text{ m}$$

$$N^2 = 2 \times 10^{-4} \times 980 \times 8/2250 \text{ cm} = 7 \times 10^{-4} \text{ sec}^{-1}$$

$$U = 1.5 \text{ cm/sec}$$

Inserting these values into equation (8) yields a value for the phase speed of -1.5 cm/sec which compares favorably with the observed speed. At this speed the wave would propagate across the domain of the model in 12 years.

The effects of the Rossby wave are well illustrated by the changes in the temperature contours (Figures 33 through 36). With the approach of the wave from the east, the baroclinic zone is displaced southward. While the baroclinic zone nearly returns to its original location after the wave passes, the temperature structure of the high latitudes is altered for a more extensive period. The high latitude isotherms are displaced southward and eastward; however the streamlines indicate flow from the south which should aid in returning the isotherms to their previous configuration.

The Rossby wave is therefore considered to be a transient feature
due to the sudden insertion of salinity into the model and the salinity's
dynamical effects on the currents. As the wave slowly propagates across
the basin, its amplitude decreases due to the lateral eddy diffusion in
the model. The e-folding time scale for damping is of the order of
$[(k^2 + l^2) A_H]^{-1}$, where A_H is the lateral eddy diffusion for heat. With
$A_H \sim 10^7$ cm^2/sec, the time scale for damping is of the order of 5-10 years.
Thus it appears that another 5-10 years of model integration will perhaps
be necessary in order to allow the large-scale geostrophic currents to
completely adjust to the new dynamical constraints imposed by the salinity
field. This is not considered a serious problem.

With the dynamical effects of the salinity reasonably well defined,
the convective adjustment parameterization discussed in the prior section
was inserted into the model. Within 40 days of simulated time the tempera-
tures exceeded the F6.2 format. The individual terms of equation (7) were
rechecked to insure their magnitudes and signs were correct. All terms
produced appropriate values for realistic salinities, depths and tempera-
tures; however, in the presence of strong surface cooling at high latitudes
during the winter of year 253-254, unrealistic sea temperatures were
generated. Temperatures below -3°C caused $\frac{\partial \sigma}{\partial T}$ to become positive which
forced the neutral value of $\frac{\partial T}{\partial Z}$ to become large and positive. The para-
meterization of convection permitted temperatures below -3°C; however,
the equation of state does not hold for temperatures below -3°C and does
not model the change of phase from water to ice which occurs at subzero
temperatures.

While distilled water reaches maximum density before freezing, sea
water with salinities greater than 25% exhibit increasing density with

25

decreasing temperature throughout the cooling process; therefore, super-cooled water continues to be convectively mixed (Sverdrup et al., 1942). Should the water column become supercooled through its entire depth, an ice cover would form insulating the column against further heat loss.

The convective adjustment parameterization was altered to prevent the instabilities previously encountered. Water cooled below -2°C was convectively mixed so as to conserve heat but maintain minimum temperatures at or above -2°C. Should the entire column cool to -2°C no further cooling would occur. With these changes inserted, the model was run through a simulated winter. Surface temperatures rapidly dropped to -2°C at the higher latitudes and were consistently cooler than the underlying layers, the stratification being provided by the imposed salinity. Because low temperatures have little effect on density, changes in the circulation patterns were not noted. The inclusion of a convective adjustment process dependent on depth and salinity as well as temperature allows cold anomalies to exist and more accurately models the physical (convective) processes observed in the high latitude ocean during winter.

V. CONCLUSIONS

The inclusion of a prescribed salinity cross section into the model produced limited changes in the large-scale ocean circulation patterns. The most significant change was the appearance of a cyclonic gyre in the northwest portion of the domain. While its seasonal fluctuation at the surface is due to atmospheric forcing, the local salinity maximum below 125 meters induced cyclonic shear at this latitude. No cyclonic gyre was formed in the region of the Gulf of Alaska presumably due to the reduced magnitude of the cyclonic atmospheric forcing in the northeast portion of the domain. The lack of bottom topography and of irregular boundaries may also impede the formation of an Alaskan gyre since all cyclonic vorticity, which is put into that region by the wind, is free to propagate westward all the way to the western boundary.

The propagation of an internal Rossby wave across the mid-latitudes altered circulation and isotherm patterns; however, these changes were of a nonpermanent nature. The effect of dissipative forces were apparent after six years. Based on the prescribed value of the lateral eddy diffusion coefficient of 5×10^7 cm^2/sec, the Rossby wave will be dissipated in approximately 10 years.

The convective adjustment parameterization allows negative temperature profiles to exist when balanced by a stabilizing salinity profile. To prevent supercooling of the surface layers, a simplistic mixing and ice formation parameterization was required. Although reasonable results were obtained, a more thorough investigation of the process of vertical convective mixing at freezing temperatures is recommended.

Several problems were encountered because the model extends to 65°N. Geographically, the Pacific Ocean above 60°N can not be realistically represented by a basin 4 kilometers deep with a width of 90° longitude. Salinity data above 60°N are sparse and highly variable since land runoff and ice formation or melting significantly alters the salinity profile there. For these reasons, 60°N would be a more appropriate northern boundary for the model.

While the inclusion of salinity in the model did not generate all the desired results, it has improved the model in specific areas. The inclusion of salinity and the improved convective adjustment process are logical progressions in the formulation of realistic ocean models which can be effectively used in the study of large-scale ocean dynamics.

APPENDIX A

DETAILS OF THE CONVECTIVE
ADJUSTMENT PARAMETERIZATION

The empirical equation of state formulated by Friedrich and Levitus (1972) is given by:

$$\sigma(S,T,Z) = C_1 + C_2T + C_3S + C_4T^2 + C_5ST + C_6T^3 + C_7ST^2 \ .$$

The values for the coefficients, which are polynomials in -Z (depth), are given in Table I. Note that Z is in kilometers and defined as positive downward. Changing Z to positive upward and taking the partial derivative of sigma with respect to Z yields:

$$\frac{\partial\sigma}{\partial Z} = -\frac{\partial C_1}{\partial Z} - \frac{\partial C_2}{\partial Z}T - \frac{\partial C_3}{\partial Z}S - \frac{\partial C_4}{\partial Z}T^2 - \frac{\partial C_5}{\partial Z}ST - \frac{\partial C_6}{\partial Z}T^3 - \frac{\partial C_7}{\partial Z}ST^2 \ .$$

Inserting the values for the coefficients and performing a scale analysis on the equation yields:

$$\frac{\partial\sigma}{\partial Z} = -5.1215 + .1Z + .0363T - .0016ZT + .0086S - .0002SZ$$

$$-.0006T^2 - .0002ST + \ldots$$

$$= -5.1215 \ (10^{-3} \ gm/cm^3 \ km)$$

$$= -5.1215 \times 10^{-5} (10^{-3} \ gm/cm^3 \ cm) \ .$$

Likewise, the differentiation and scale analysis for sigma with respect to S is given by:

$$\frac{\partial\sigma}{\partial S} = C_3 + C_5T + C_7T^2$$

$$= .8056 + .0086Z + .0001Z^2 - .0030T - .0002ZT + \ldots$$

$$= .8056 \ (10^{-3} \ gm/cm^3 \%) \ ;$$

however, the expression for the change in sigma with respect to T can not be simplified to a single value through scale analysis. Retaining all terms which may be significant over the expected range of temperature, salinity and depth, the effect of temperature on density is given by:

$$\frac{\partial \sigma}{\partial T} = C_2 + 2C_4 T + C_5 S + 3C_6 T^2 + 2C_7 ST$$

$$= .0498 + .0363Z + .0008Z^2 - .0152T - .0013ZT - .003S - .0002ZS$$

$$+ .0001T^2 + .0001ST.$$

The stable lapse rate is given by:

$$\frac{\partial T}{\partial Z} \geq (-\frac{\partial \sigma}{\partial Z} - \frac{\partial \sigma}{\partial S} \frac{\partial S}{\partial Z})/\frac{\partial \sigma}{\partial T}$$

or

$$\frac{\partial T}{\partial Z} \geq (5.1215 \times 10^{-5} - .8056 \frac{\partial S}{\partial Z})/(K_1 + K_2 T + K_3 S + .0001T(T+S))$$

where

$$K_1 = .498 + .0363Z + .0008Z^2$$

$$K_2 = -.0152 - .0013Z$$

$$K_3 = -.003 - .0002Z$$

30

TABLE I. Coefficients for the Friedrich and Levitus equation of state, equation (5). $C_i = a_i + b_i Z + c_i Z^2$ where Z is in kilometers and positive downward.

i	a_i	b_i	c_i
1	-7.2169×10^{-2}	$+5.1215 \times 10^{-0}$	-5.012×10^{-2}
2	$+4.9762 \times 10^{-2}$	-3.6349×10^{-2}	$+7.853 \times 10^{-4}$
3	$+8.0560 \times 10^{-1}$	-8.5540×10^{-3}	$+1.070 \times 10^{-4}$
4	-7.5911×10^{-3}	$+6.4295 \times 10^{-4}$	-1.397×10^{-5}
5	-3.0063×10^{-3}	$+1.9365 \times 10^{-4}$	-3.899×10^{-6}
6	$+3.5187 \times 10^{-5}$	-3.9740×10^{-6}	-5.695×10^{-8}
7	$+3.7297 \times 10^{-5}$	-2.8108×10^{-6}	$+1.147 \times 10^{-7}$

TABLE II. Coefficients for the Friedrich and Levitus equation of state, equation (4). $C_i = a_i + b_i Z + c_i Z^2$ where Z is in kilometers and positive downward.

i	a_i	b_i	c_i
1	-9.2163×10^{-2}	$+5.1140 \times 10^{-0}$	-4.692×10^{-2}
2	$+4.3314 \times 10^{-2}$	-3.5685×10^{-2}	$+7.689 \times 10^{-4}$
3	$+8.0640 \times 10^{-1}$	-8.6826×10^{-3}	$+1.433 \times 10^{-4}$
4	-6.2723×10^{-3}	$+5.1351 \times 10^{-4}$	-1.246×10^{-5}
5	-2.7762×10^{-3}	$+1.7792 \times 10^{-4}$	-3.985×10^{-6}

Goode's homolosine
Equal-area projection
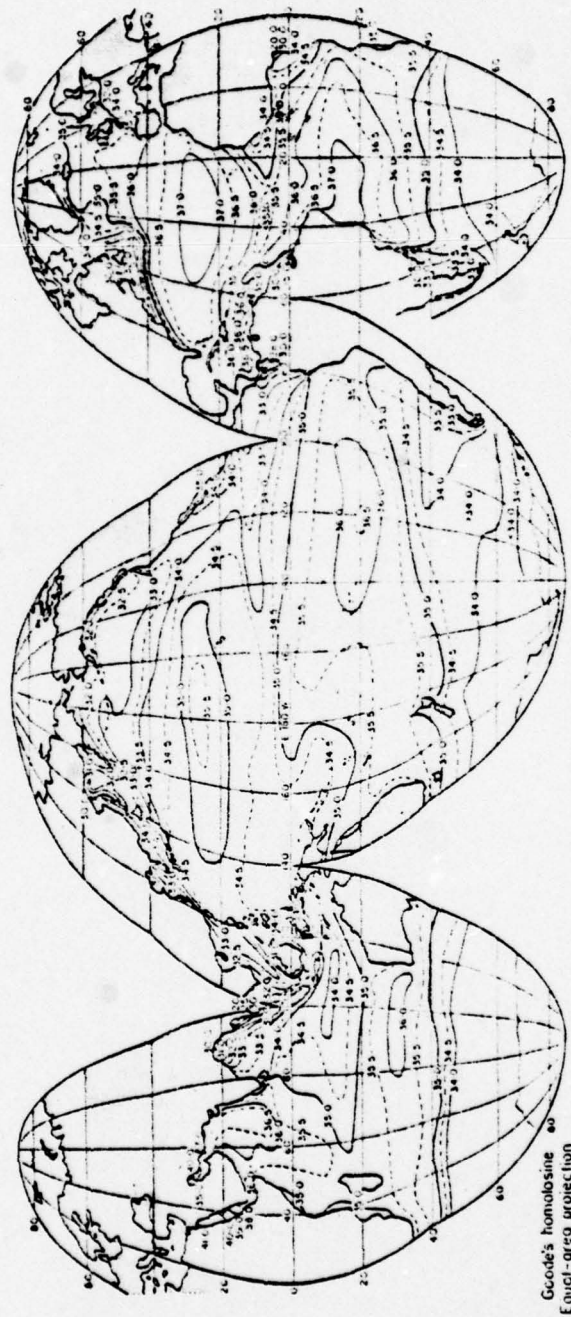
Figure 1. Surface salinity contours of the Pacific Ocean (Sverdrup et al., 1942).
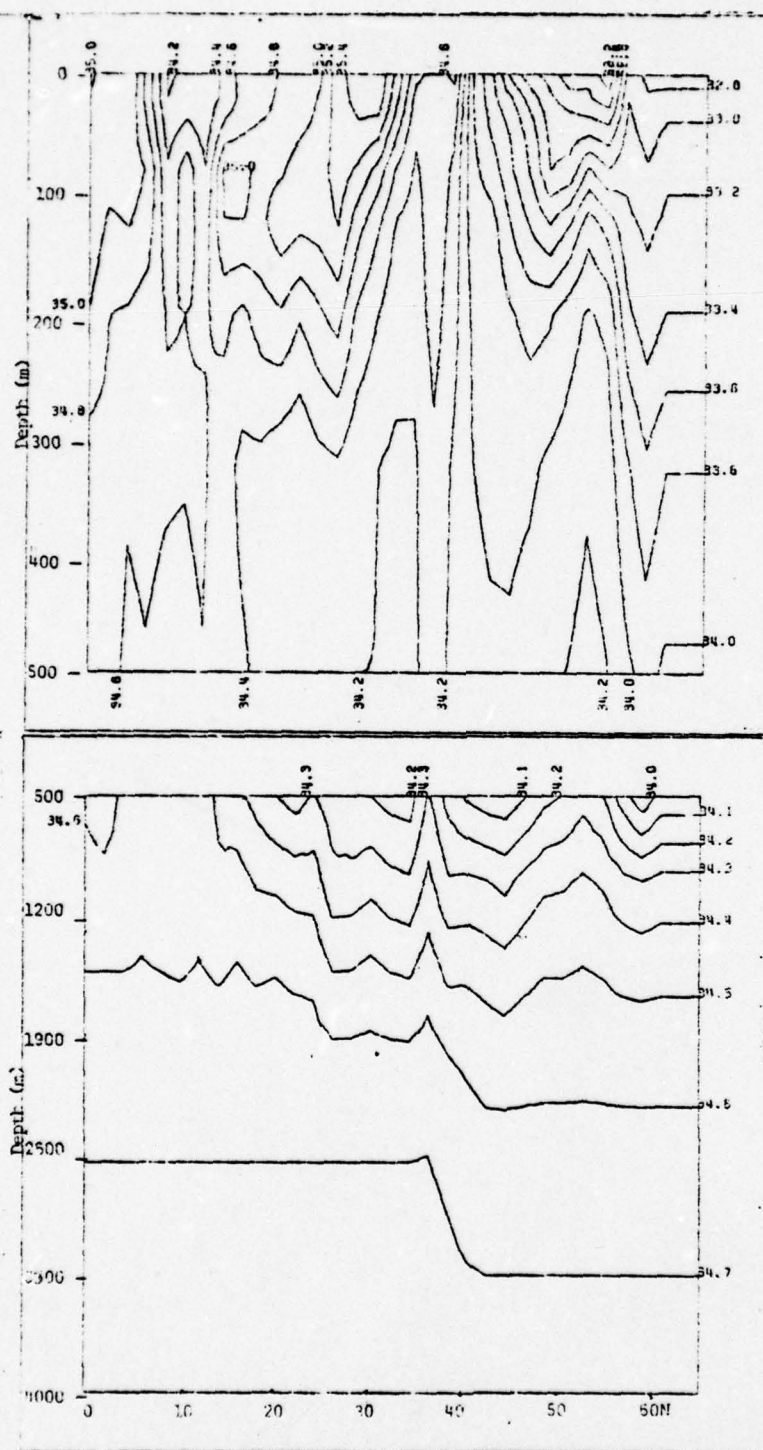
Figure 2. Salinity cross section along 160°W with no horizontal smoothing.
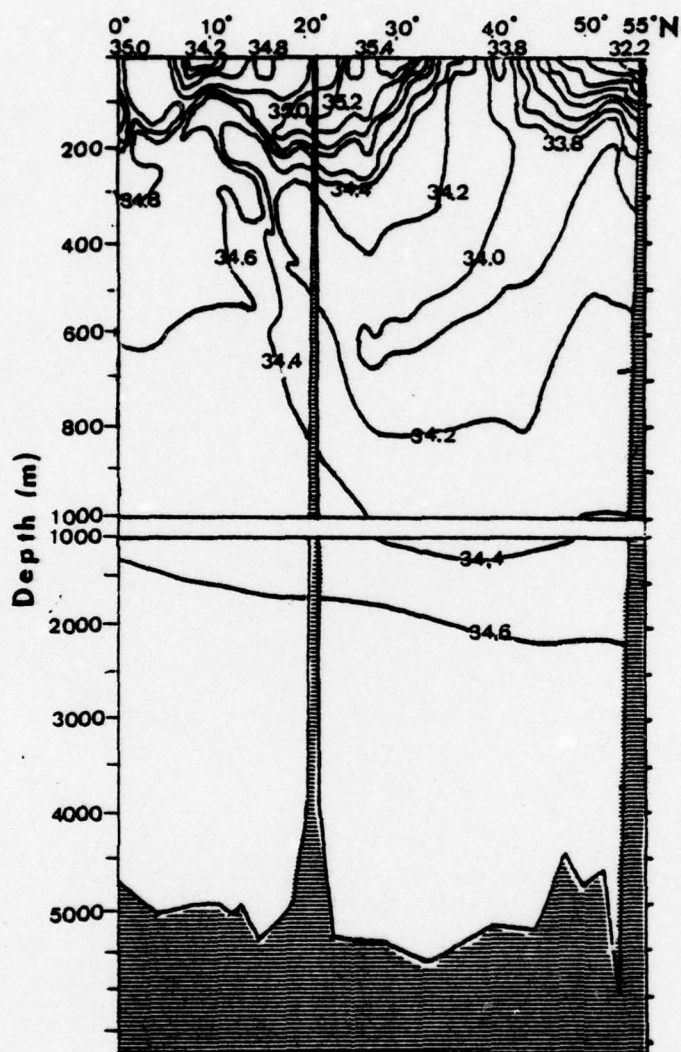
Figure 3. Salinity cross section along 160°W (Reid, 1965).
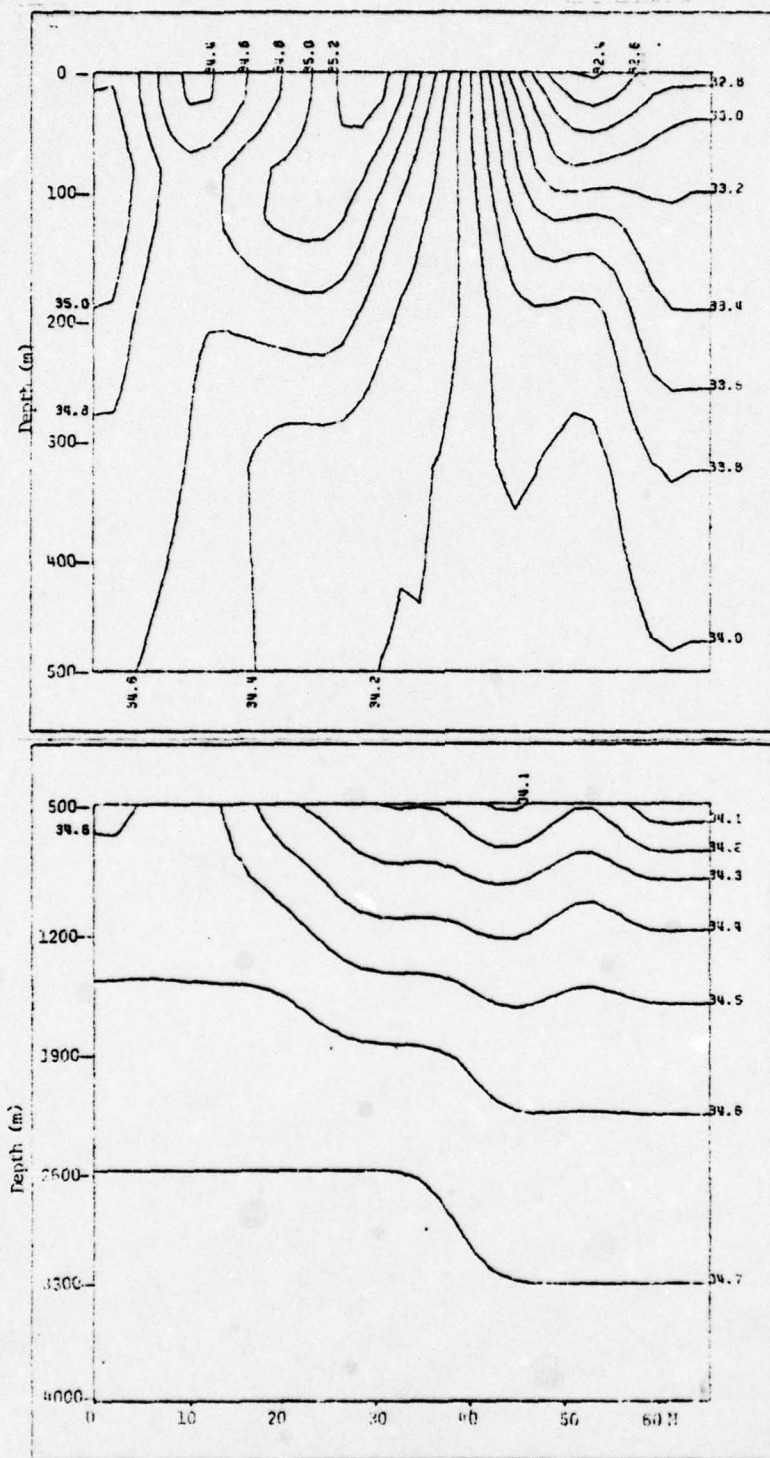
Figure 4. Salinity cross section along 160°W smoothed four times.
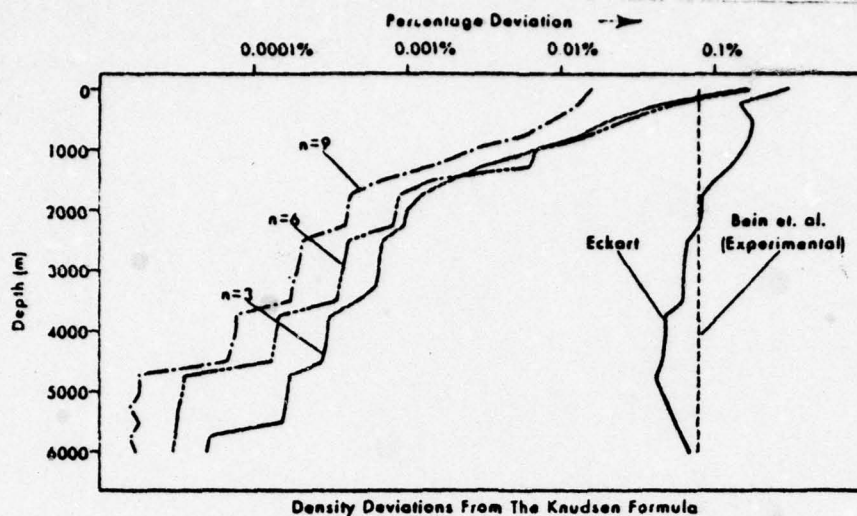
Figure 5.   Average percentage error in sigma for the Bryan and Cox equation of state where the Knudsen formula is taken as standard (Bryan and Cox, 1972).
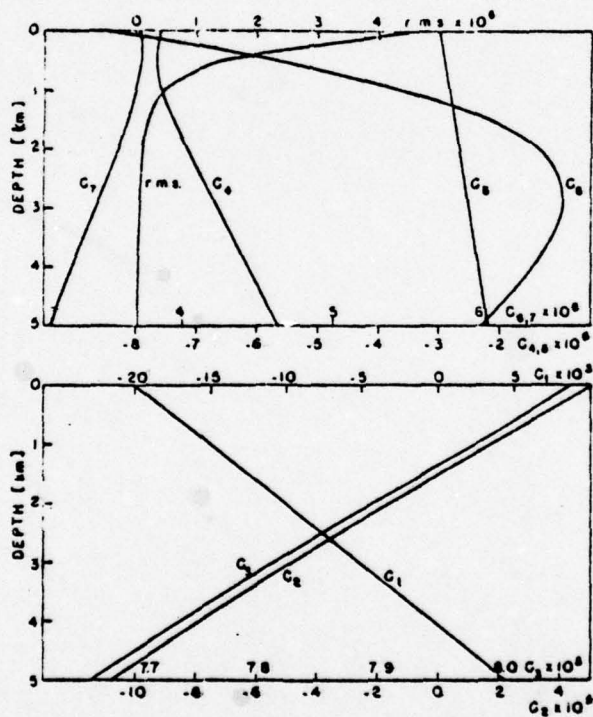
Figure 6.   Coefficients of the Friedrich and Levitus equation of state as a function of depth and rms error of this equation with respect to the Knudsen formula (Friedrich and Levitus, 1972).
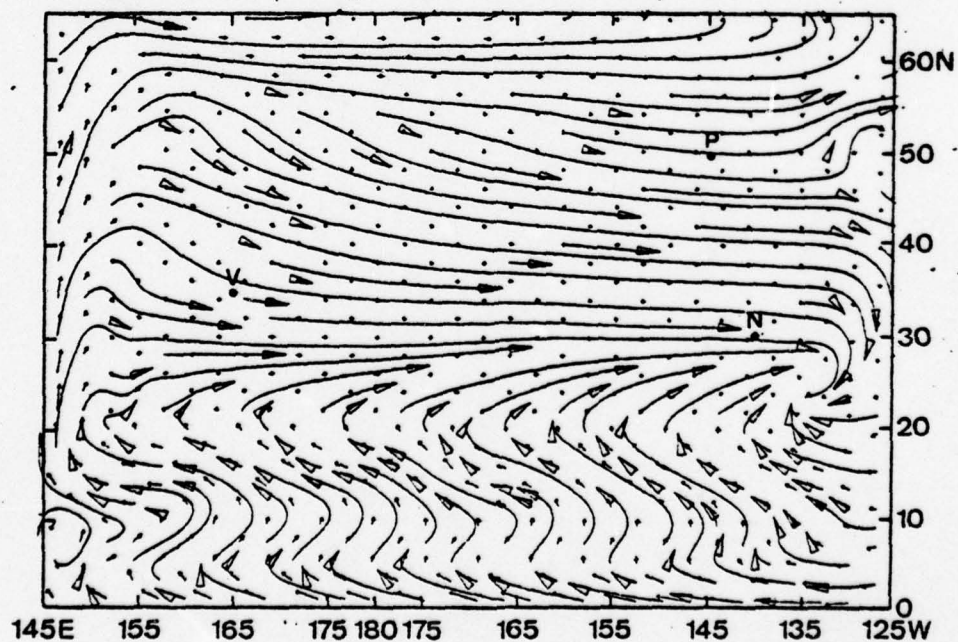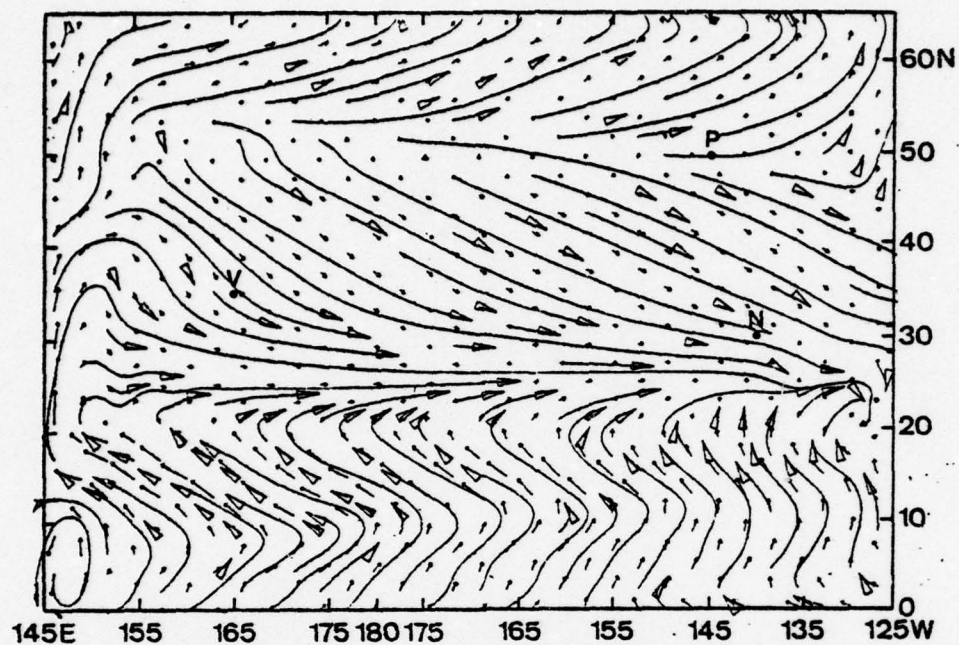
Figure 7. Streamlines and velocity vectors for surface layer, year 246
(without salinity) winter (top) and summer (bottom).
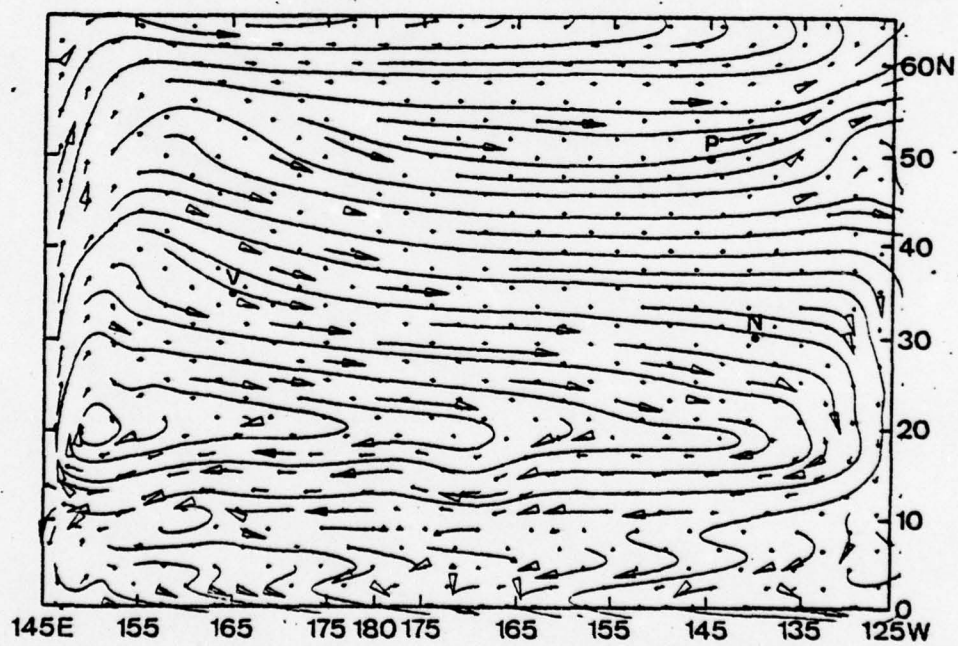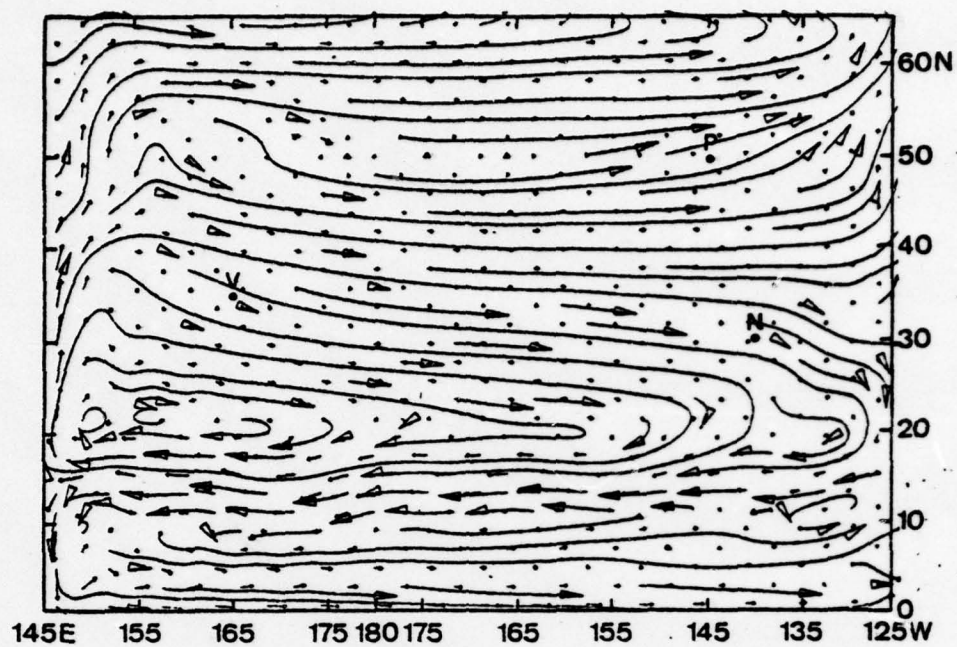
Figure 8.   Level 3 streamlines and velocity vectors
   year 246 (without salinity) winter (top) and
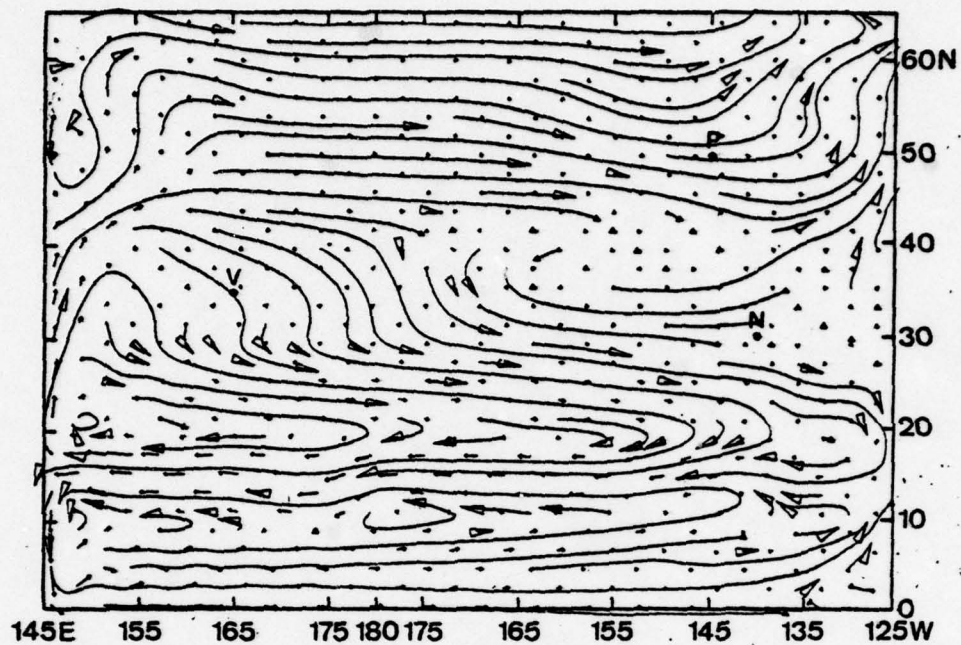   summer (bottom)
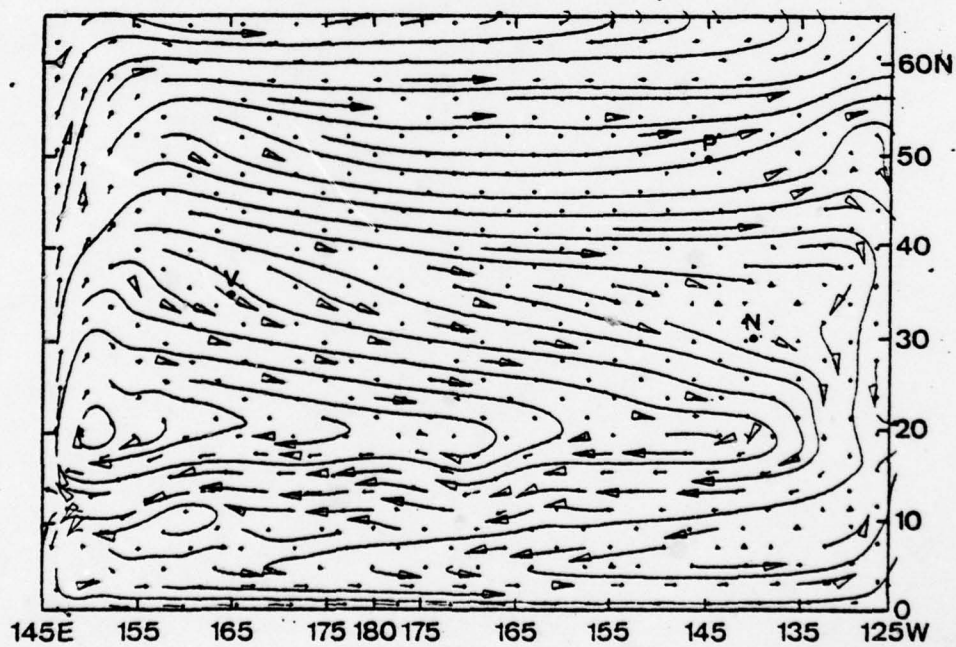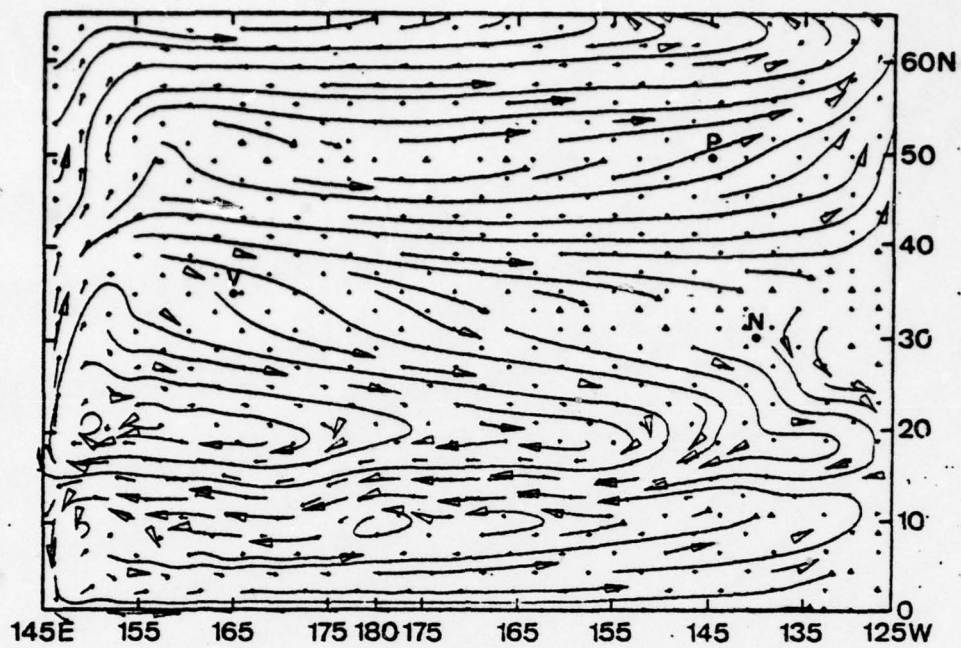
Figure 9. Level 5 streamlines and velocity vectors
year 246 (without salinity) winter (top) and
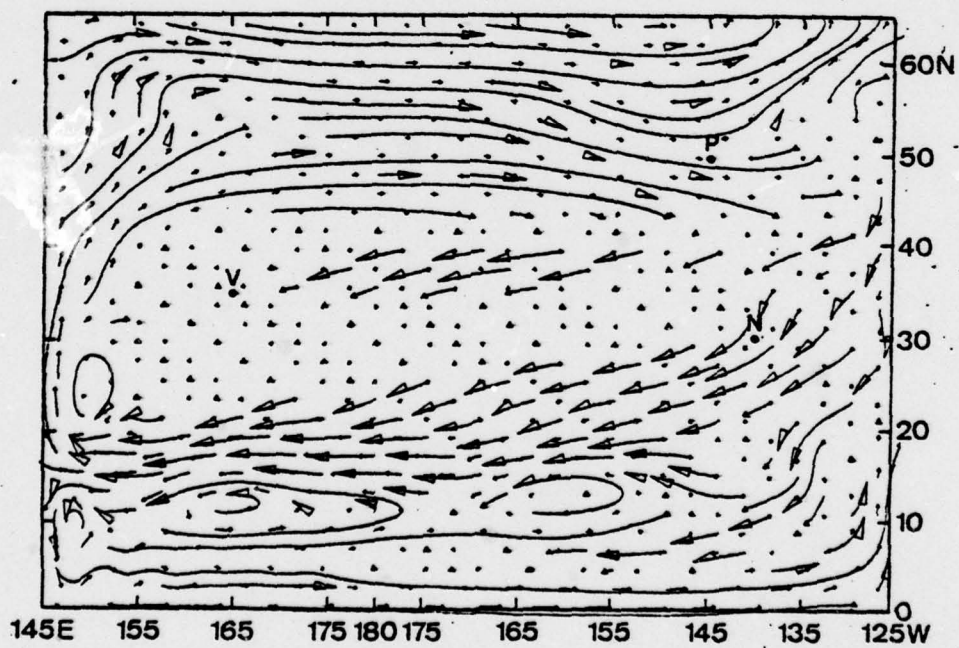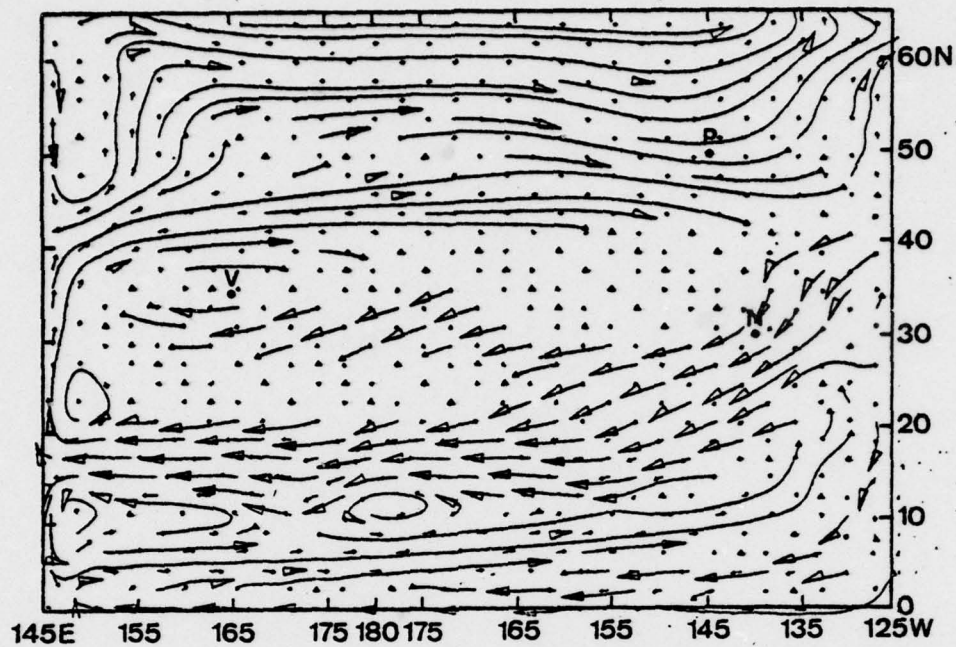summer (bottom)
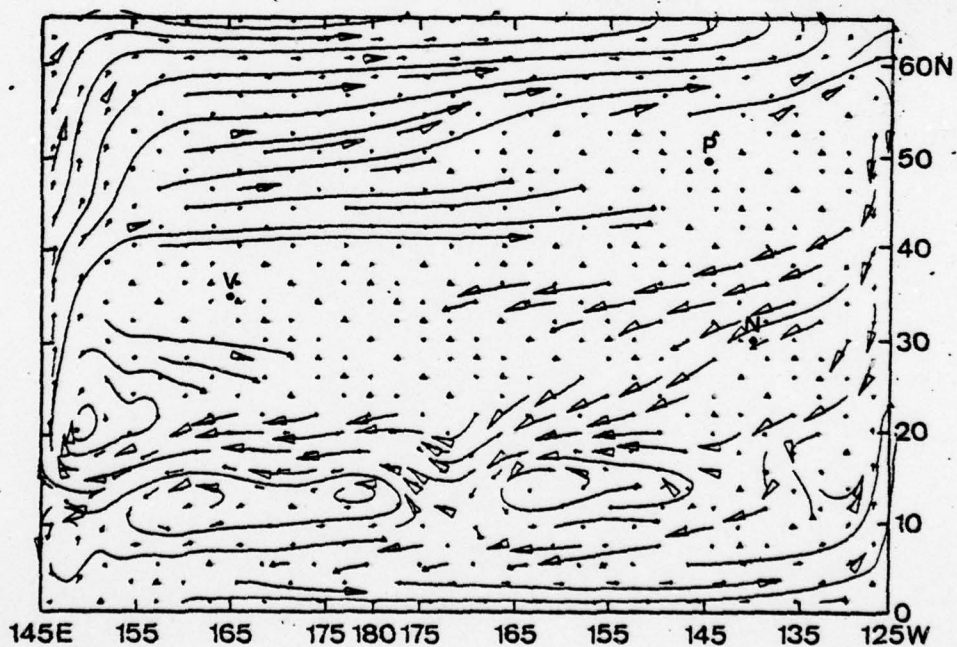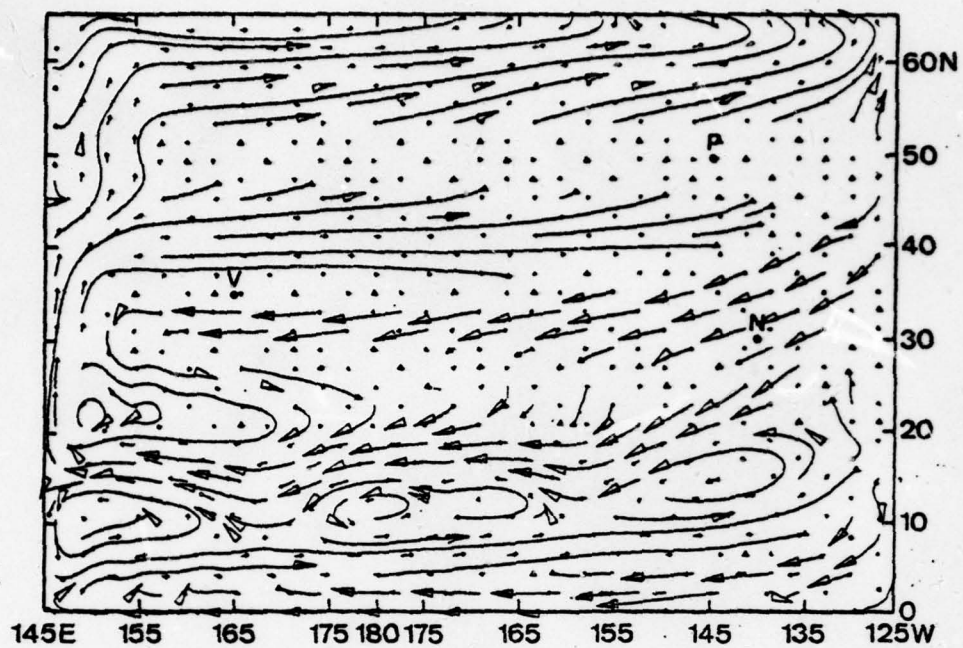
Figure 10. Level 7 streamlines and velocity vectors
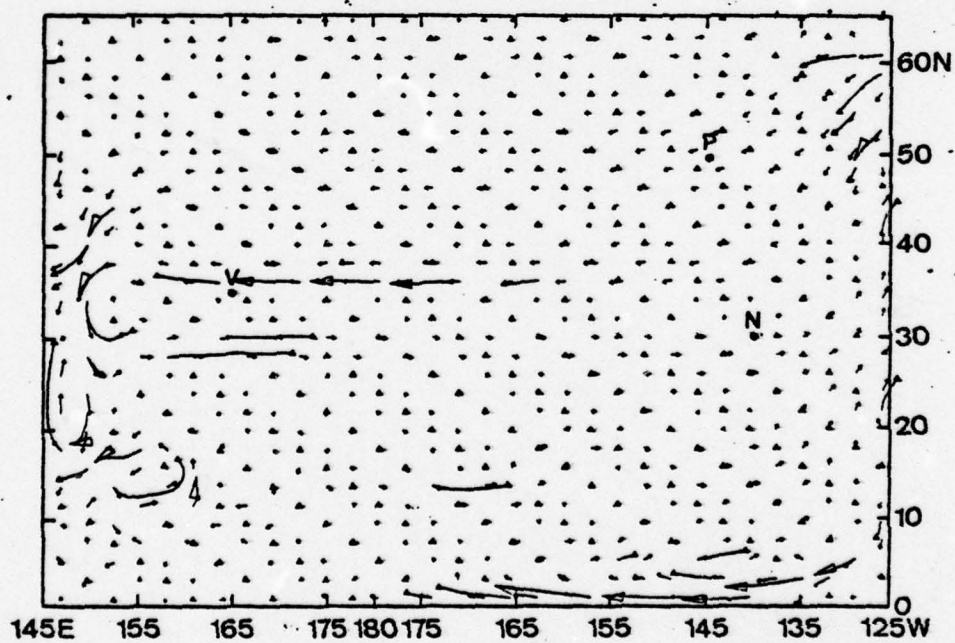year 246 (without salinity) winter (top) and
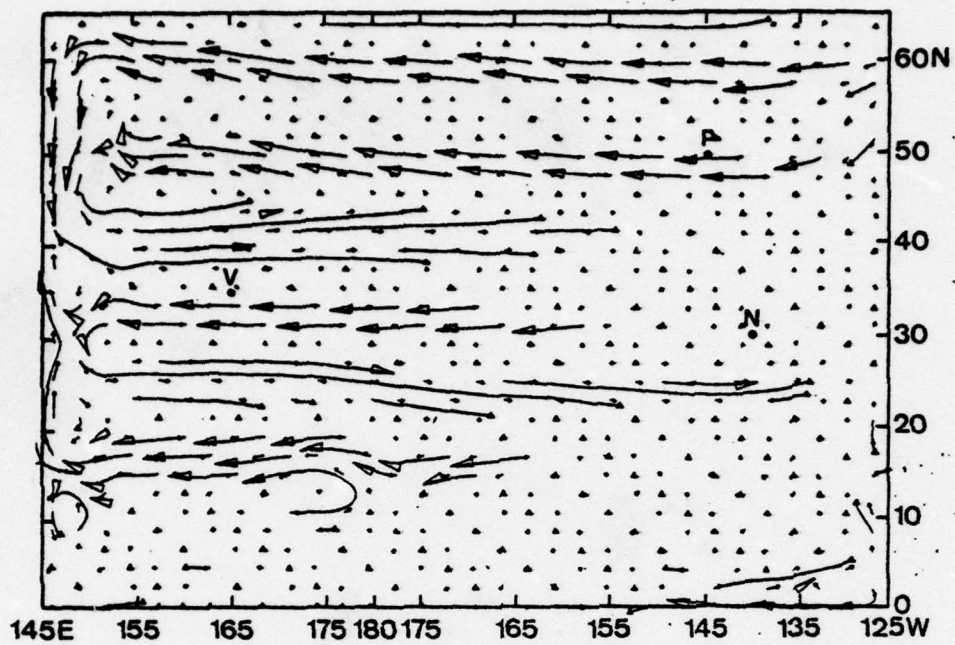summer (bottom)

40
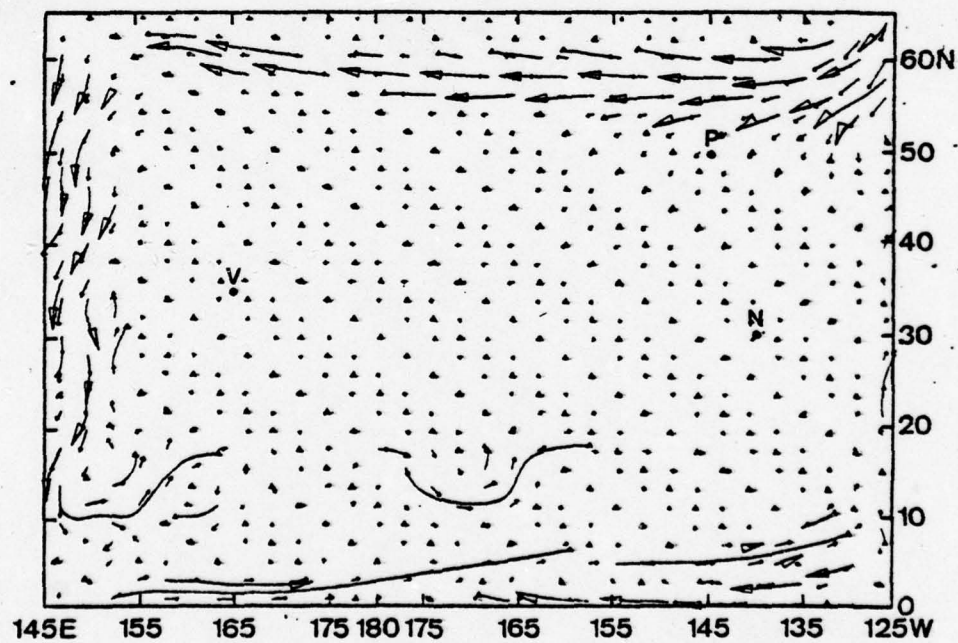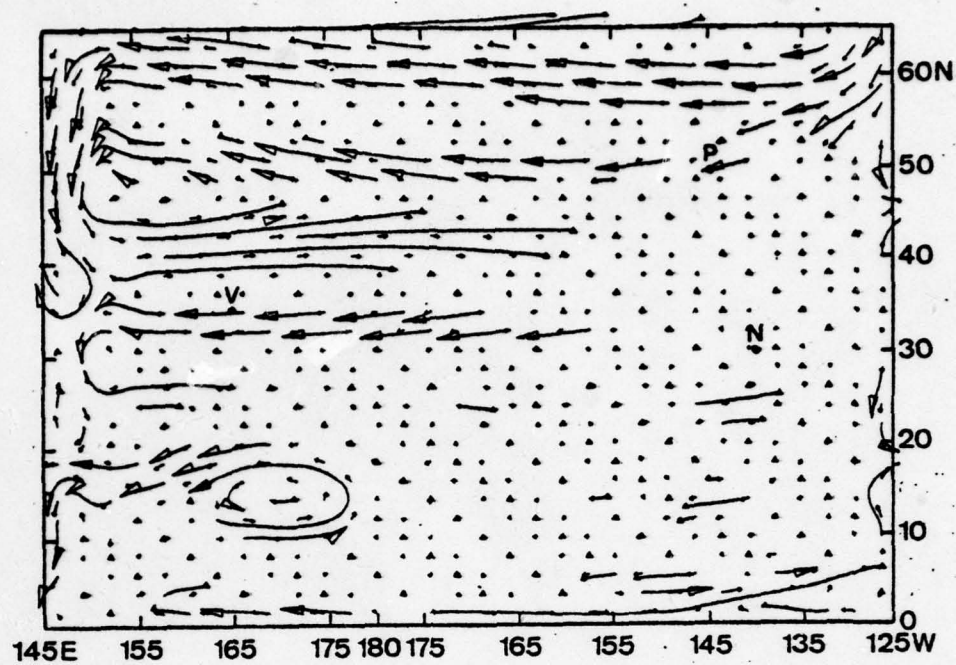
Figure 11. Level 9 streamlines and velocity vectors
year 246 (without salinity) winter (top) and
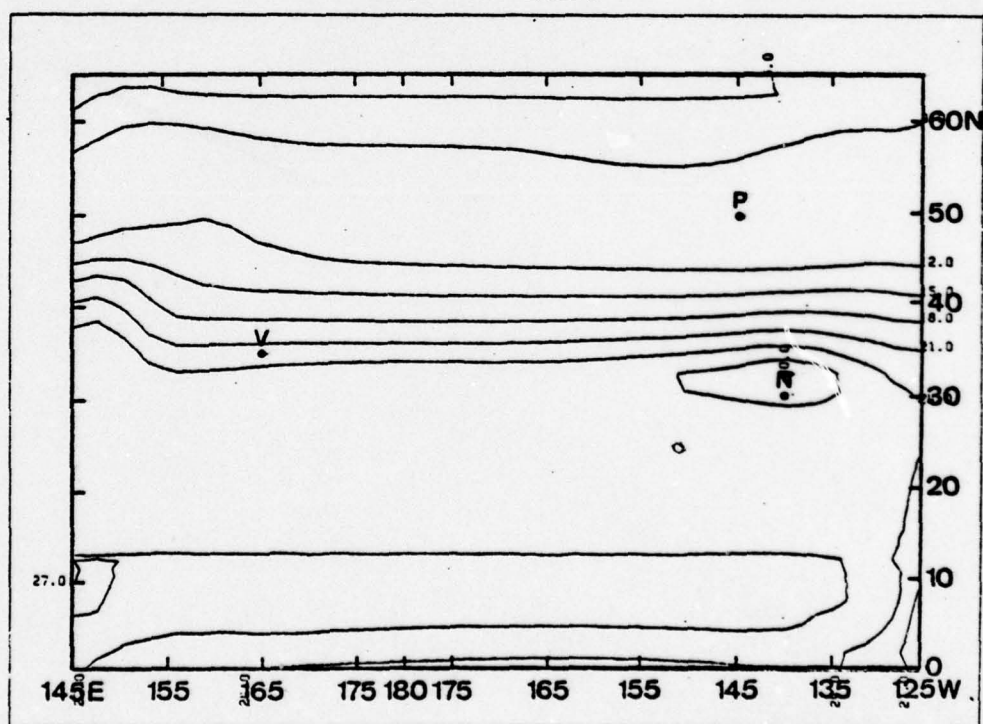summer (bottom)
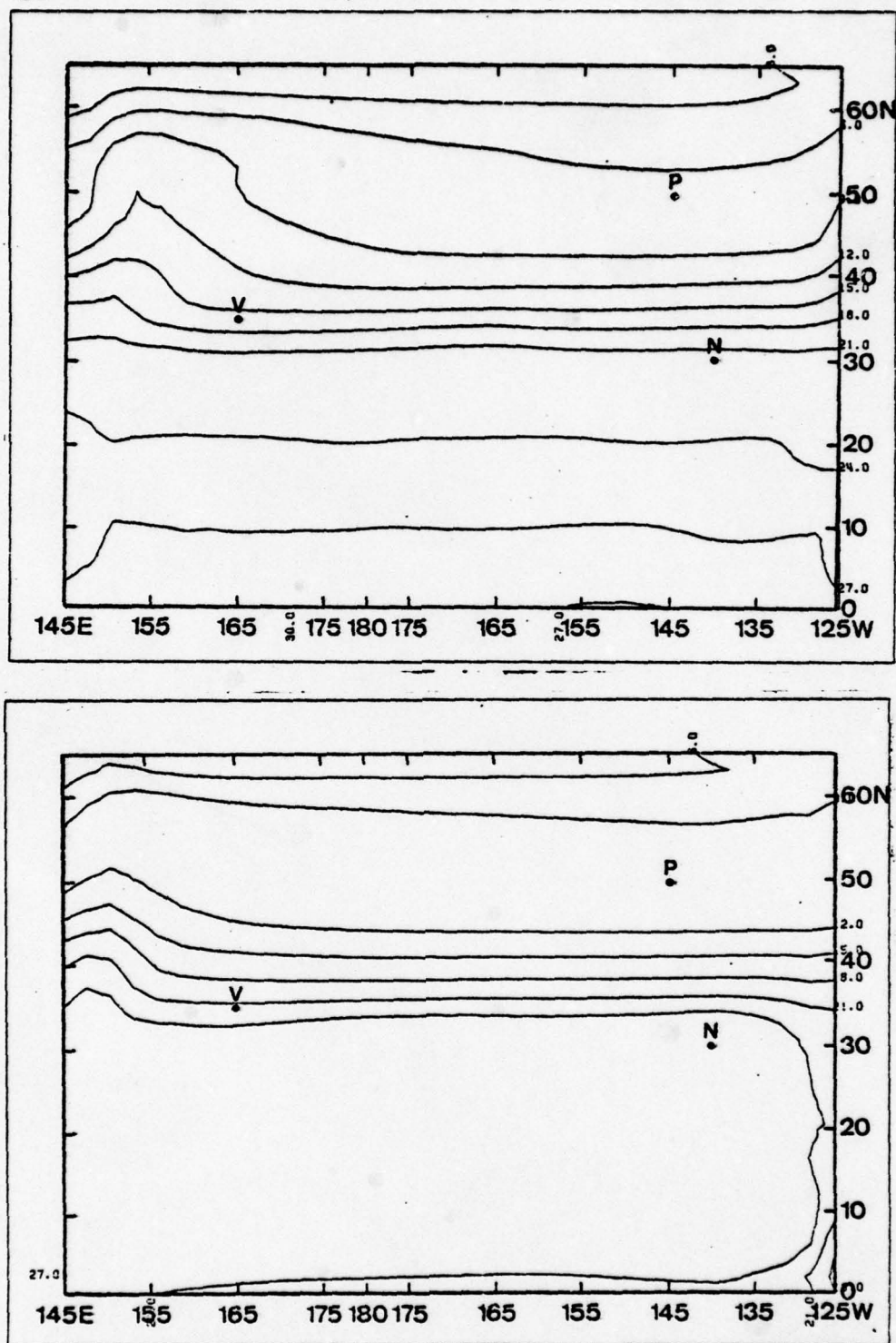
Figure 12.   Temperature contours for surface layer, year 246 (without
salinity) winter (top) and summer (bottom).
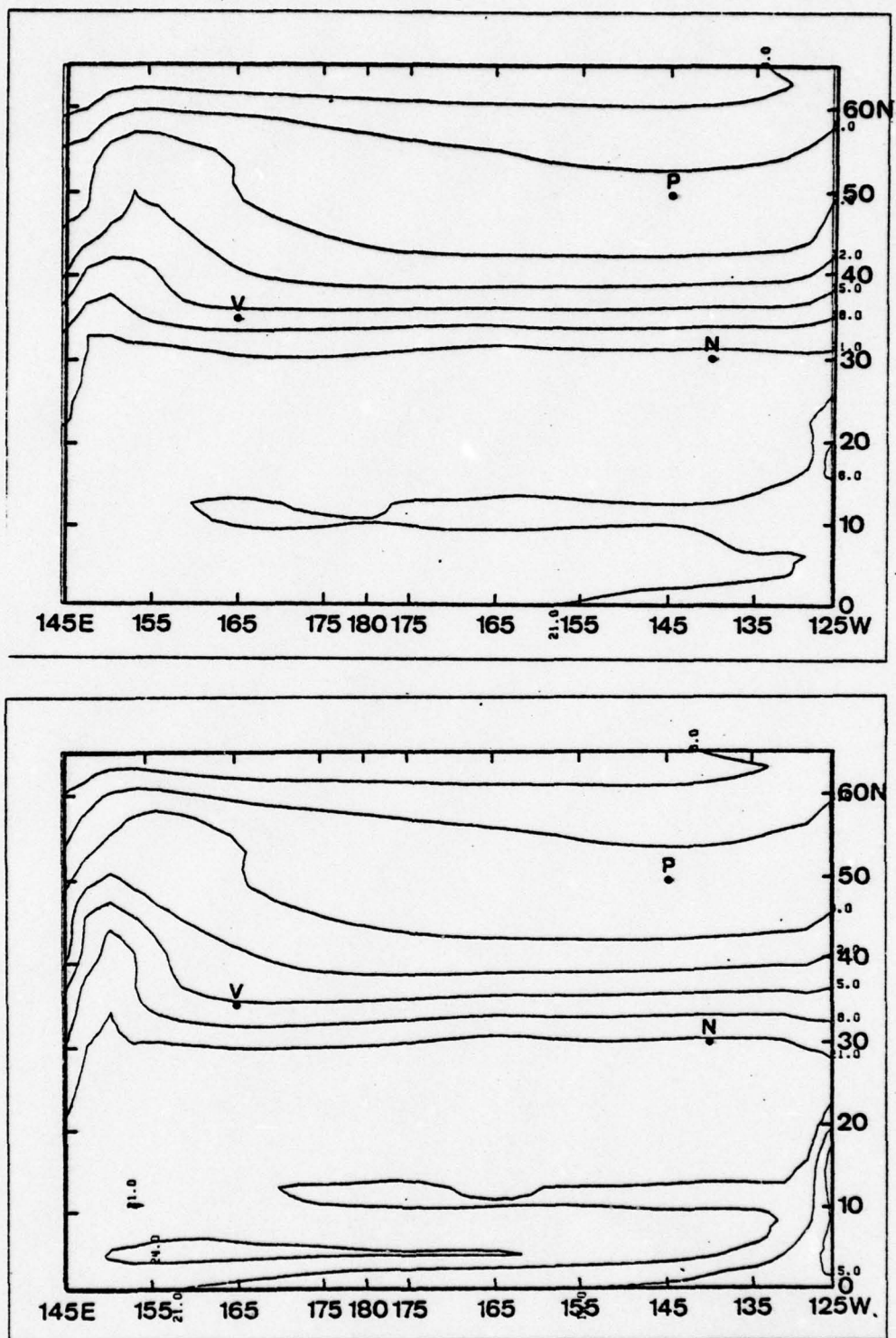
Figure 13. Level 3 temperature contours, year 246
(without salinity) winter (top) and summer (bottom)
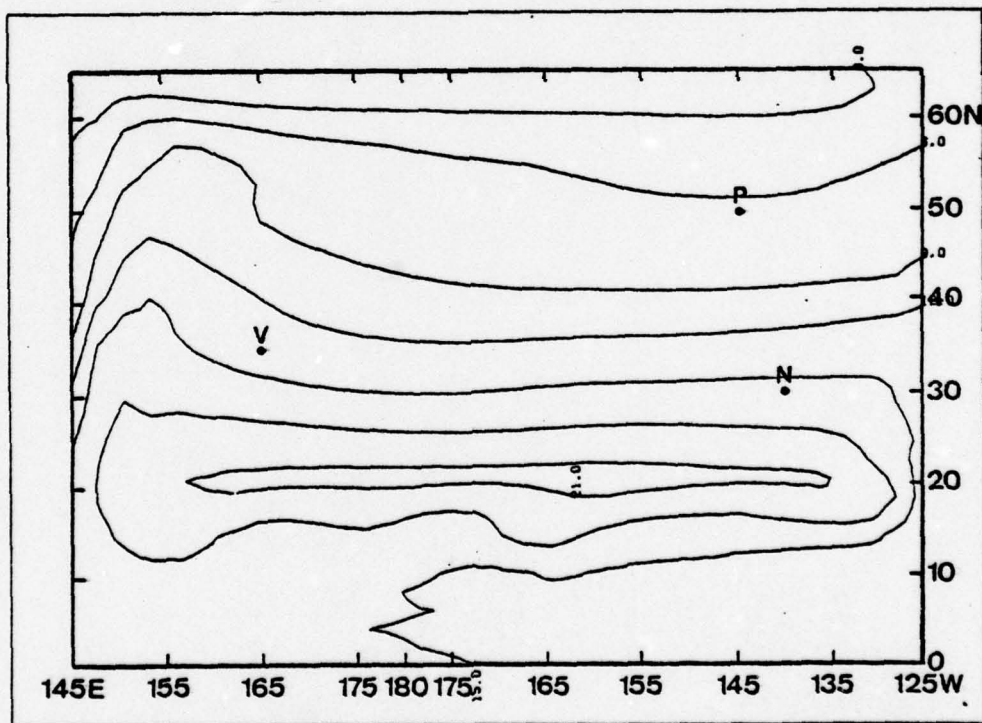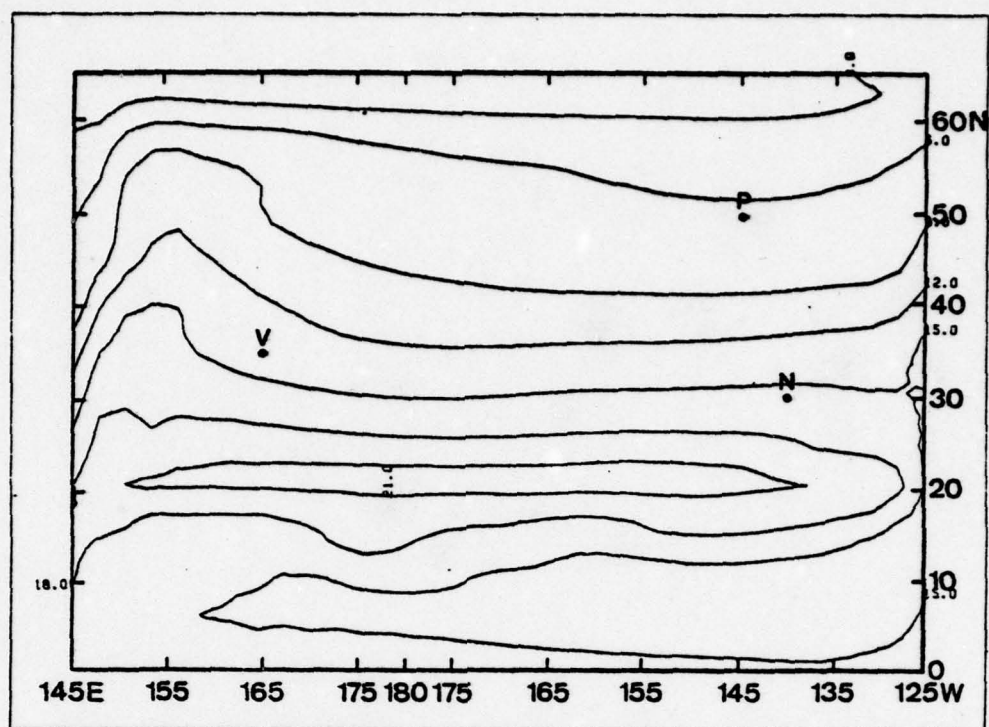
Figure 14. Level 5 temperature contours, year 246
(without salinity) winter (top) and summer (bottom)

44
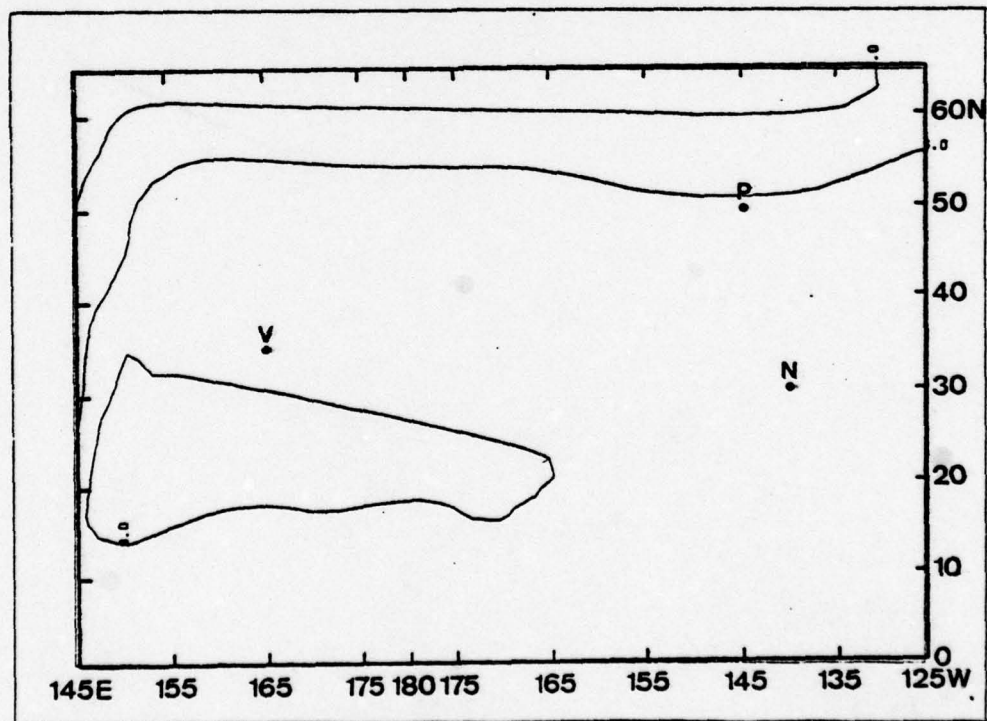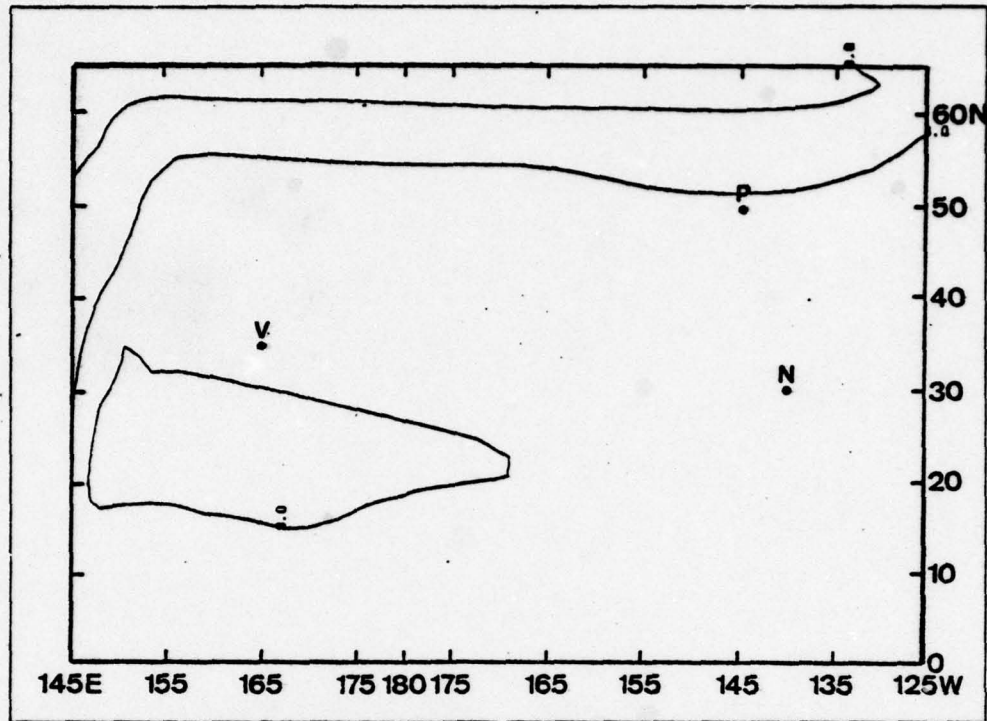
Figure 15. Level 7 temperature contours, year 246
(without salinity) winter (top) and summer (bottom)
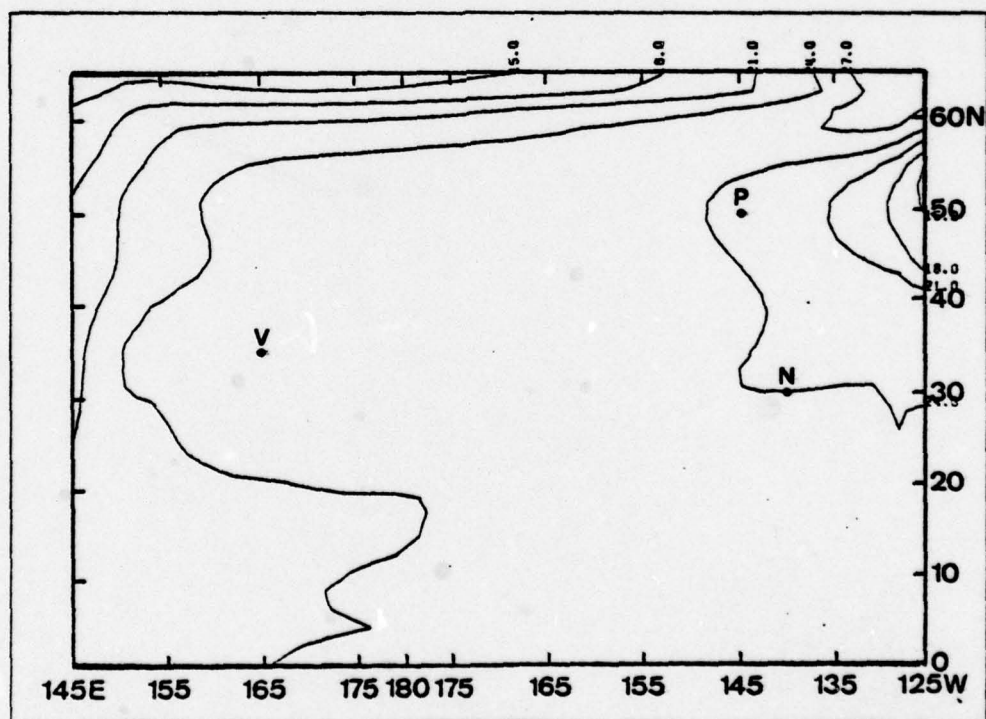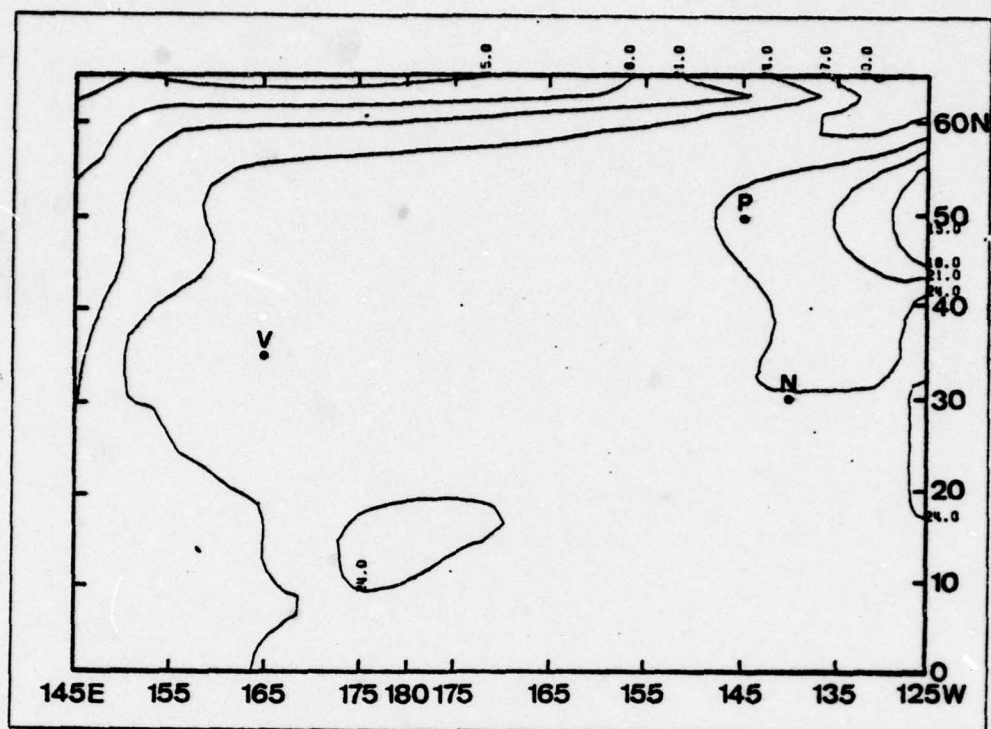
Figure 16. Level 9 temperature contours, year 246
(without salinity) winter (top) and summer (bottom)
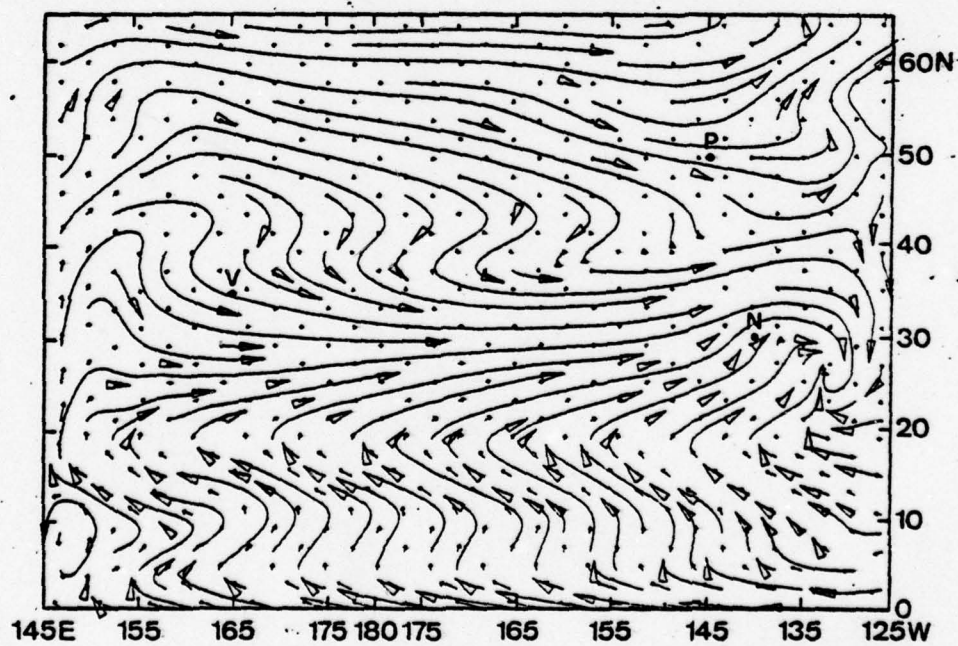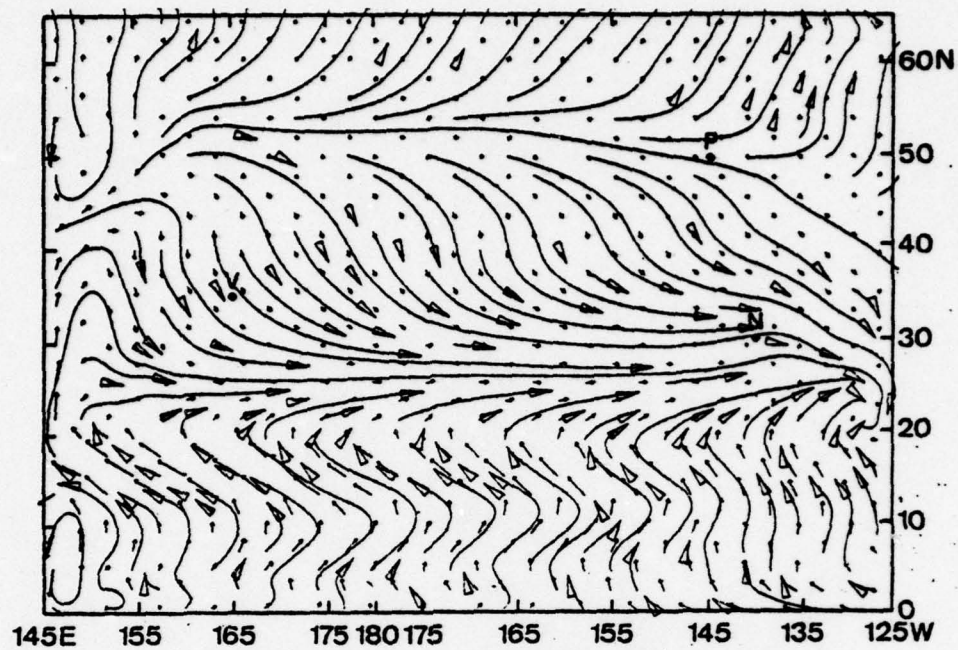
Figure 17. Surface streamlines and velocity vectors
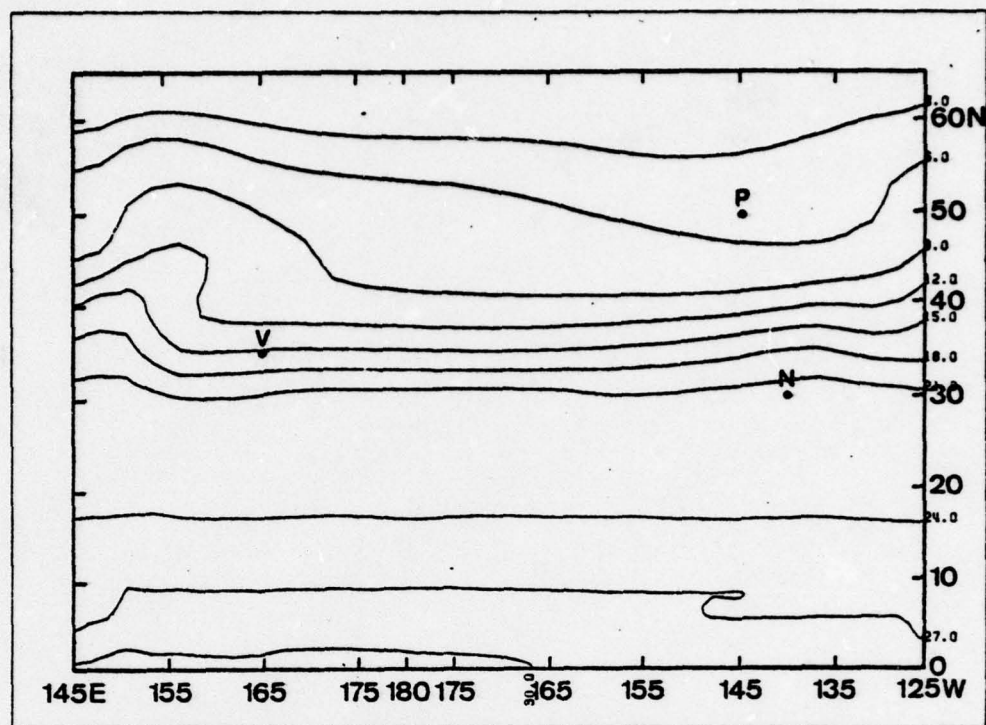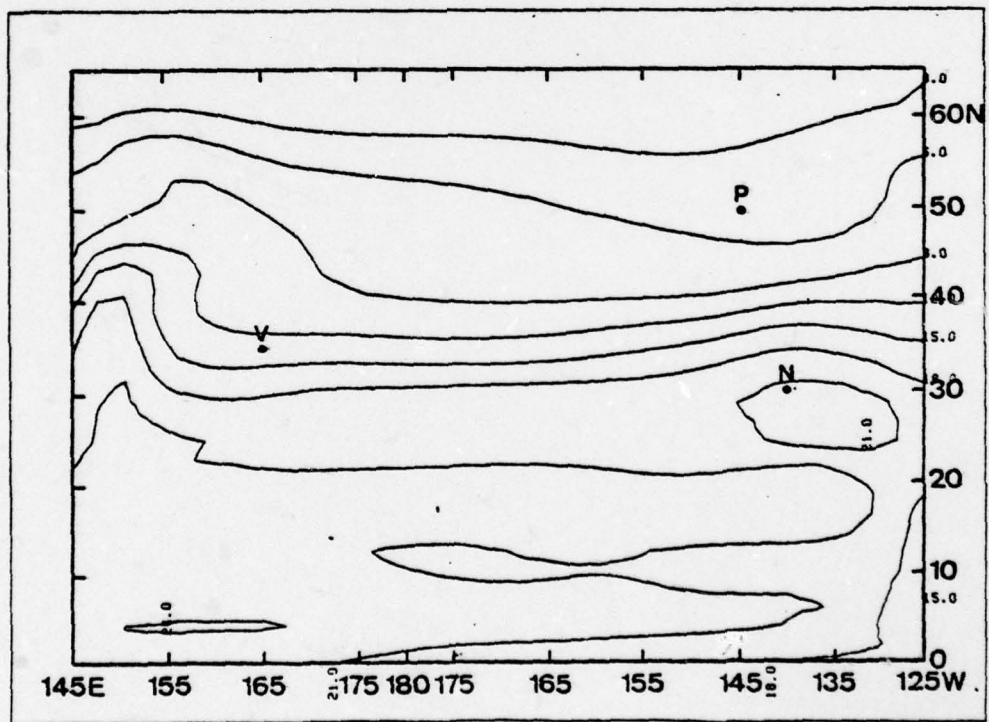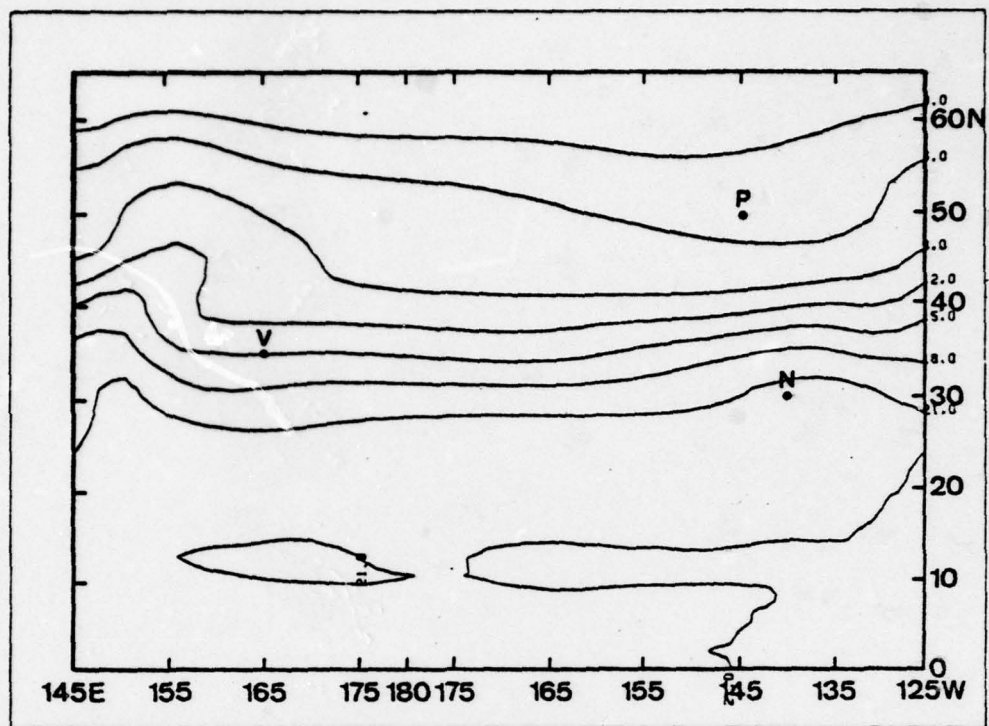year 253 (with salinity) winter (top) and
summer (bottom)
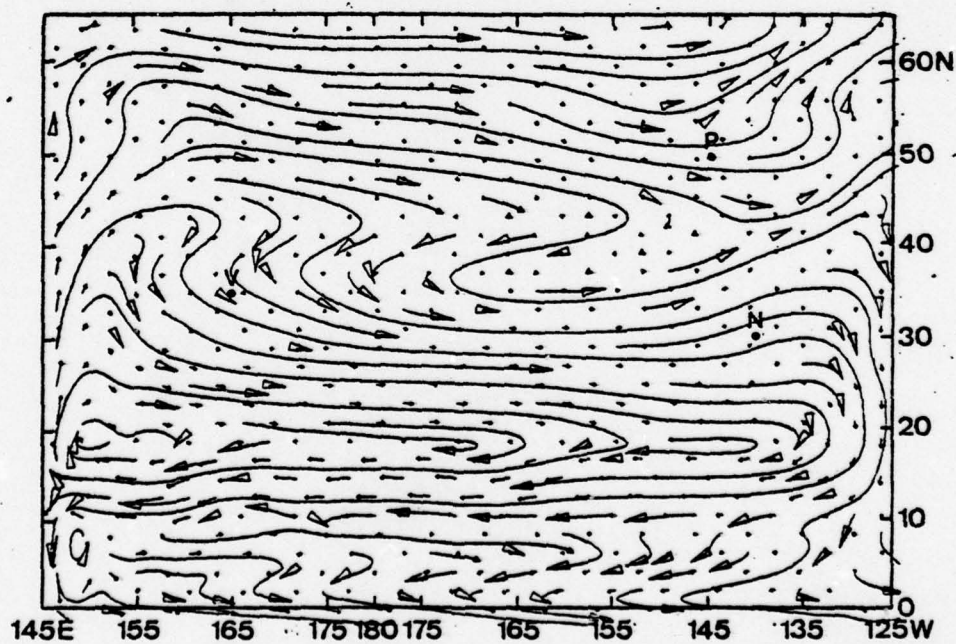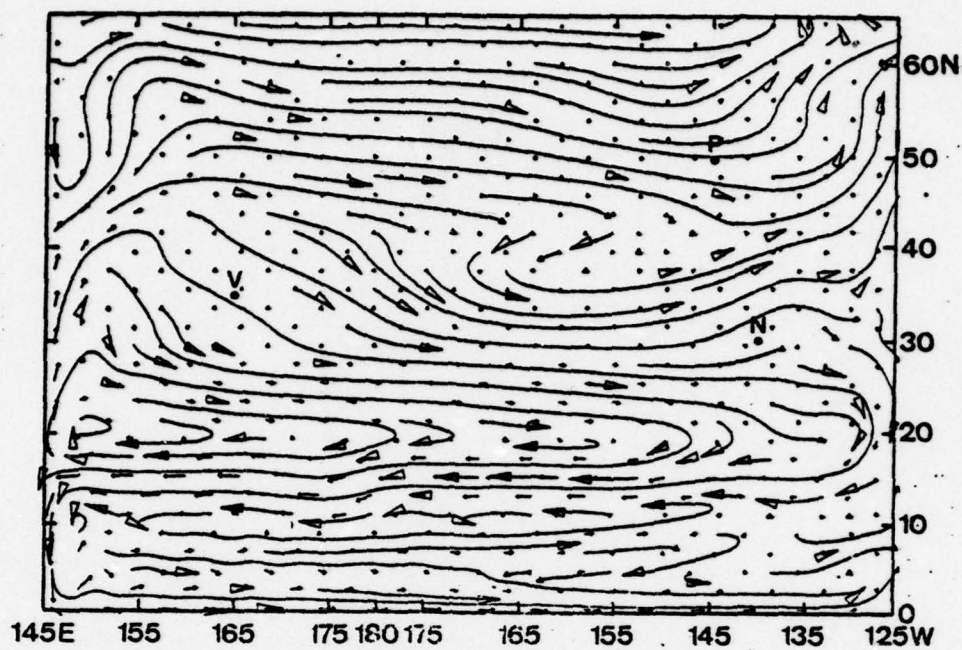
Figure 18. Level 3 streamlines and velocity vectors
year 253 (with salinity) winter (top) and
summer (bottom)
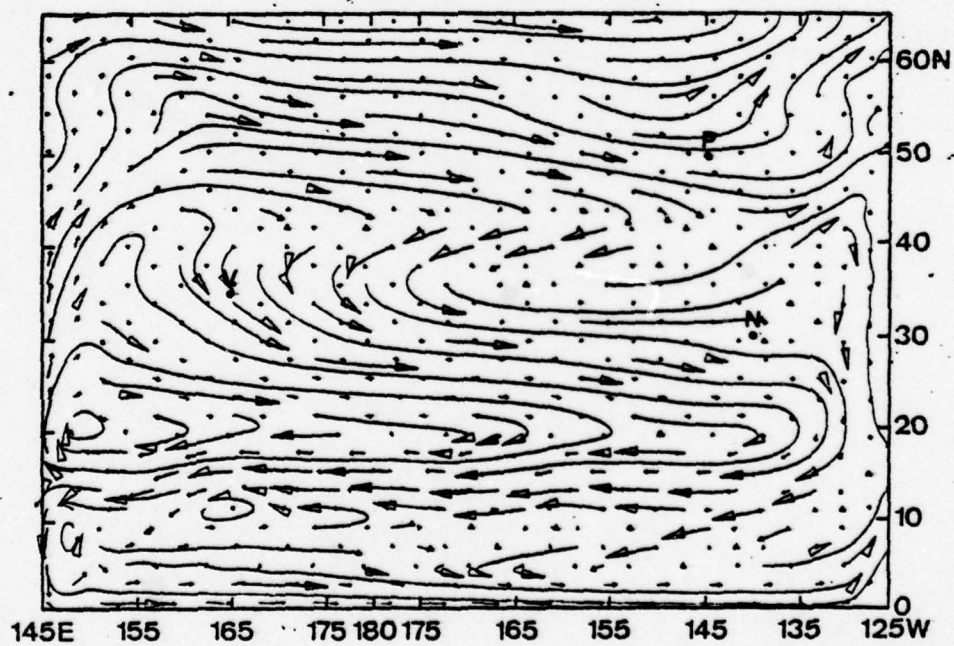
Figure 19. Level 5 streamlines and velocity vectors
year 25.3 (with salinity) winter (top) and
summer (bottom)

Figure 20. Level 7 streamlines and velocity vectors
year 253 (with salinity) winter (top) and
summer (bottom)

Figure 21. Level 9 streamlines and velocity vectors
year 253 (with salinity) winter (top) and
summer (bottom)

Figure 22. Surface temperature contours, year 253
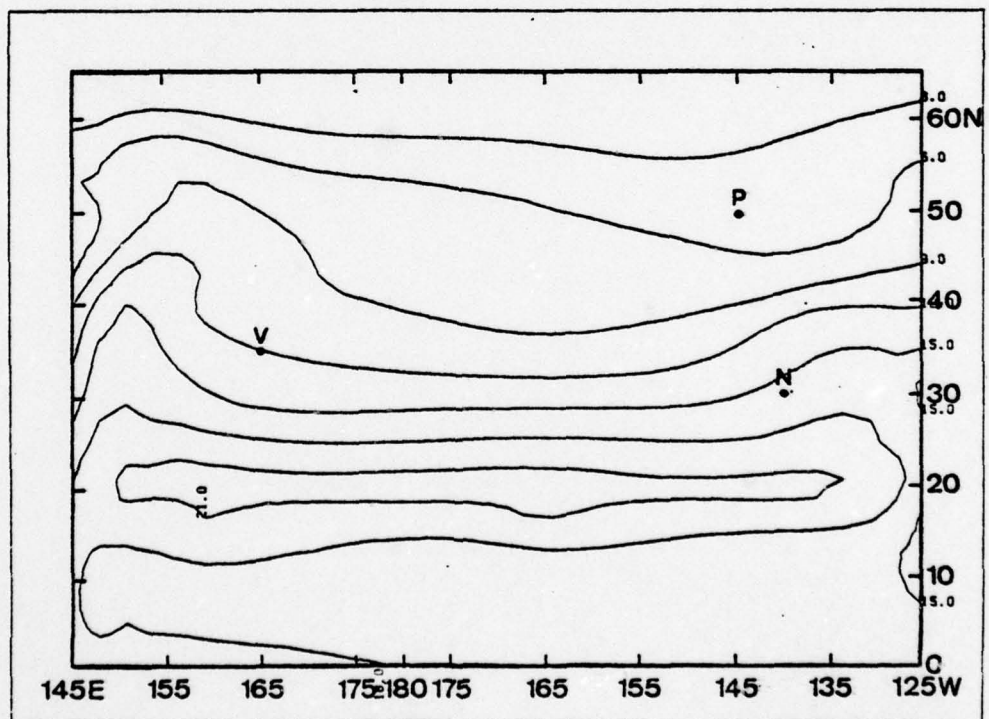(with salinity) winter (top) and summer (bottom)

Figure 23. Level 3 temperature contours, year 253
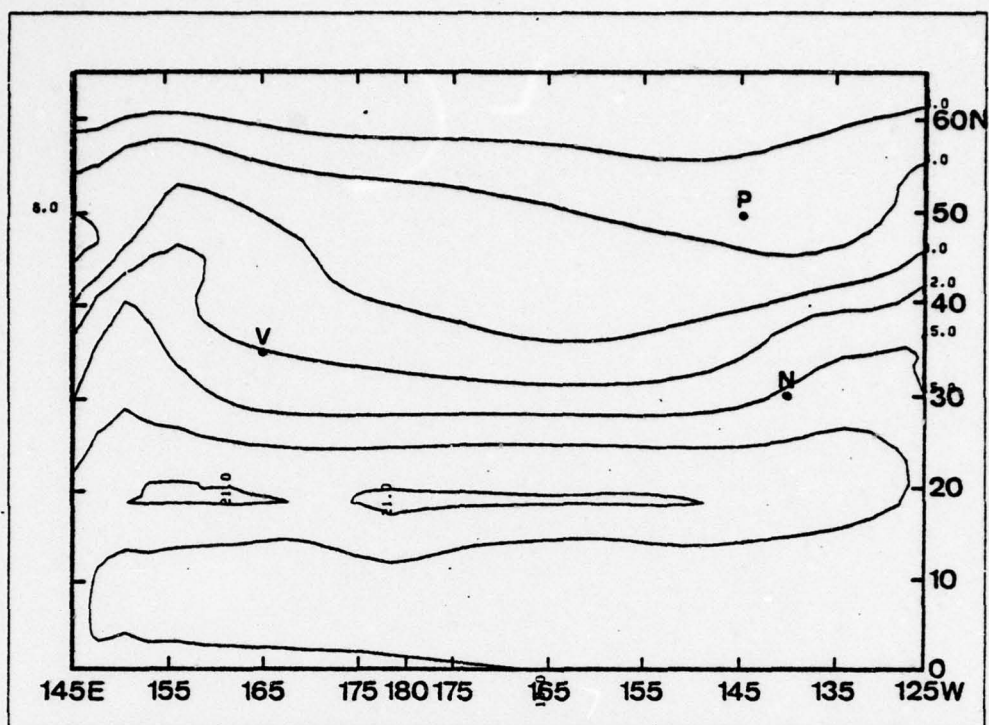(with salinity) winter (top) and summer (bottom)

Figure 24. Level 5 temperature contours, year 253
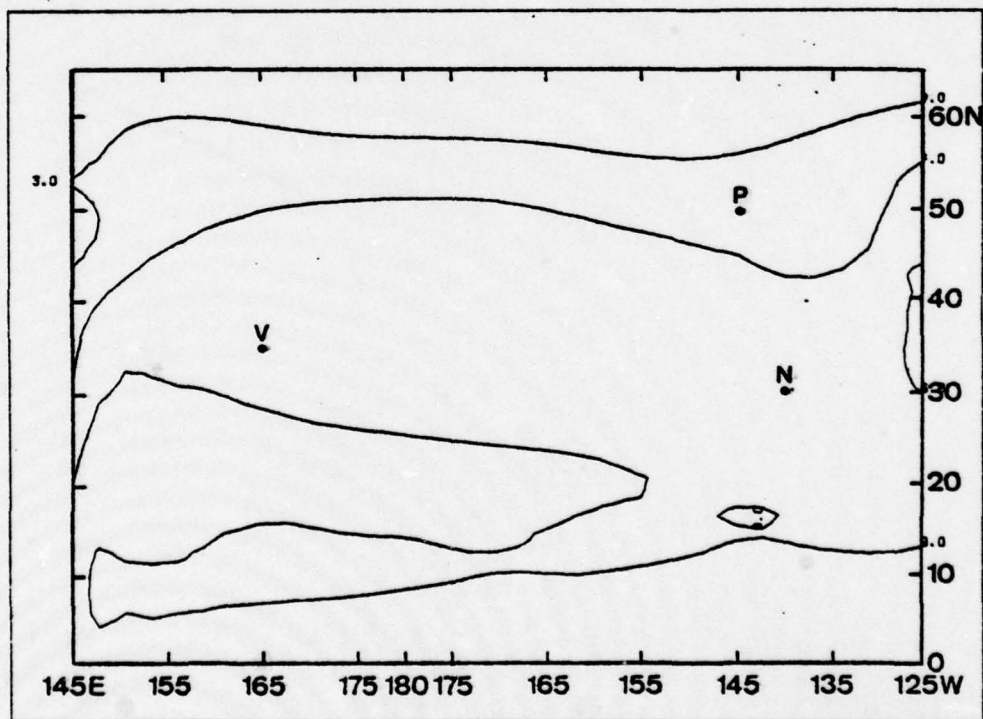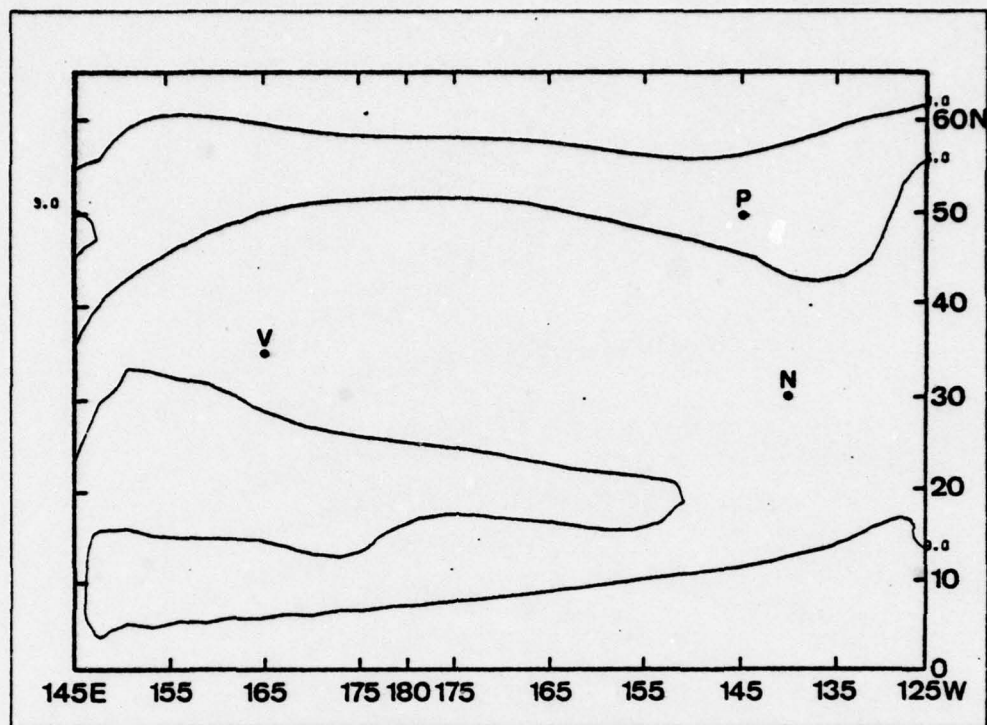(with salinity) winter (top) and summer (bottom)

Figure 25. Level 7 temperature contours, year 253
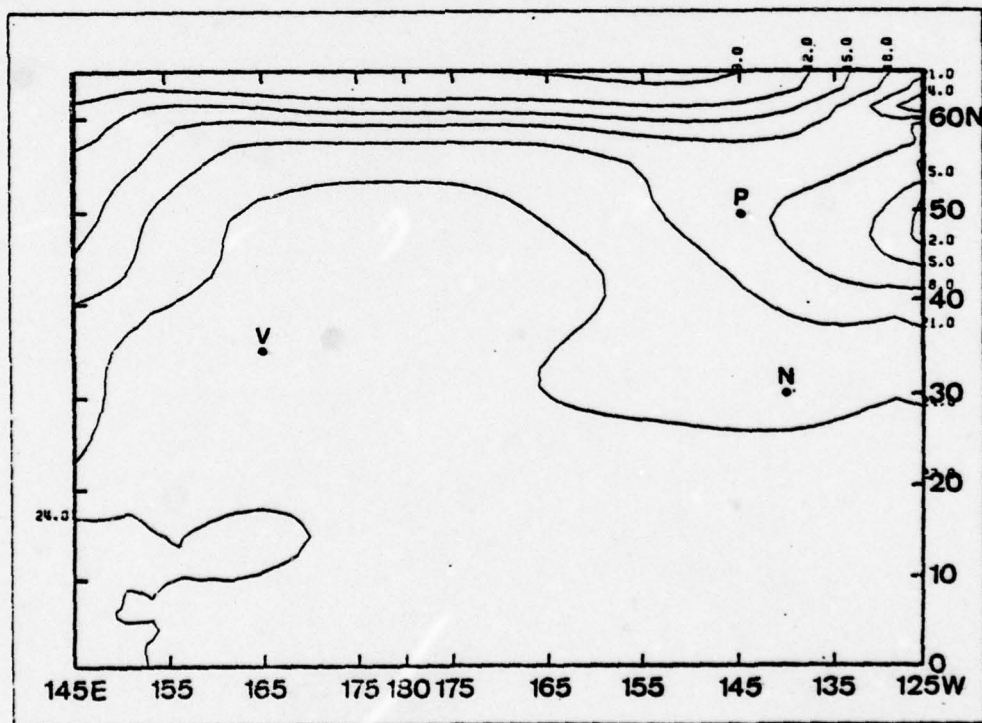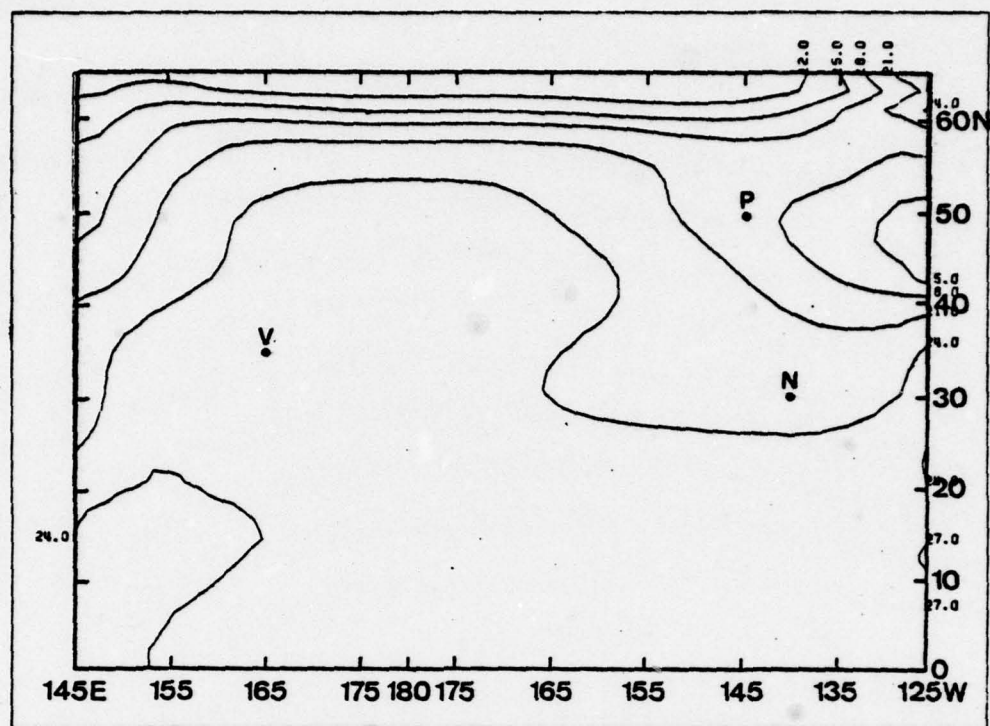(with salinity) winter (top) and summer (bottom)

55

Figure 26. Level 9 temperature contours, year 253
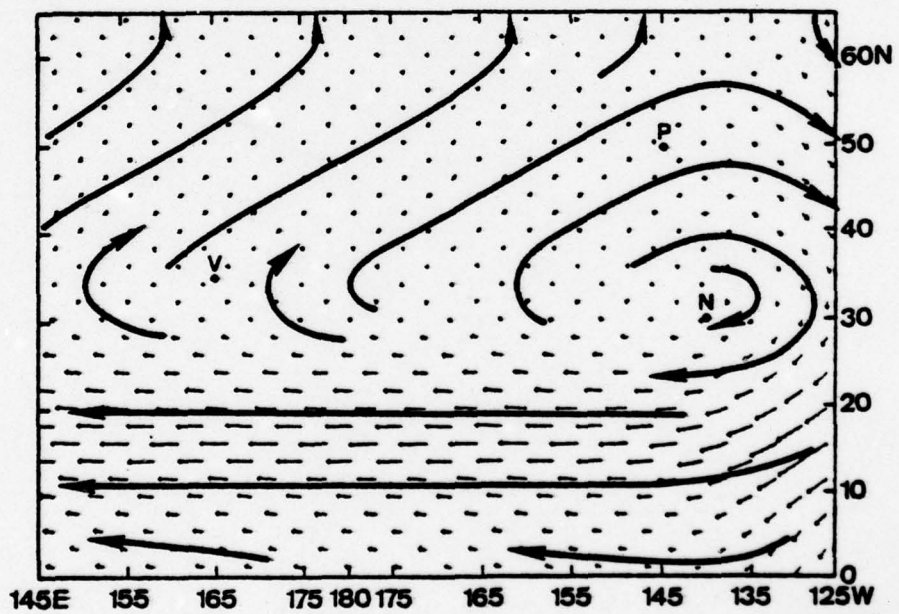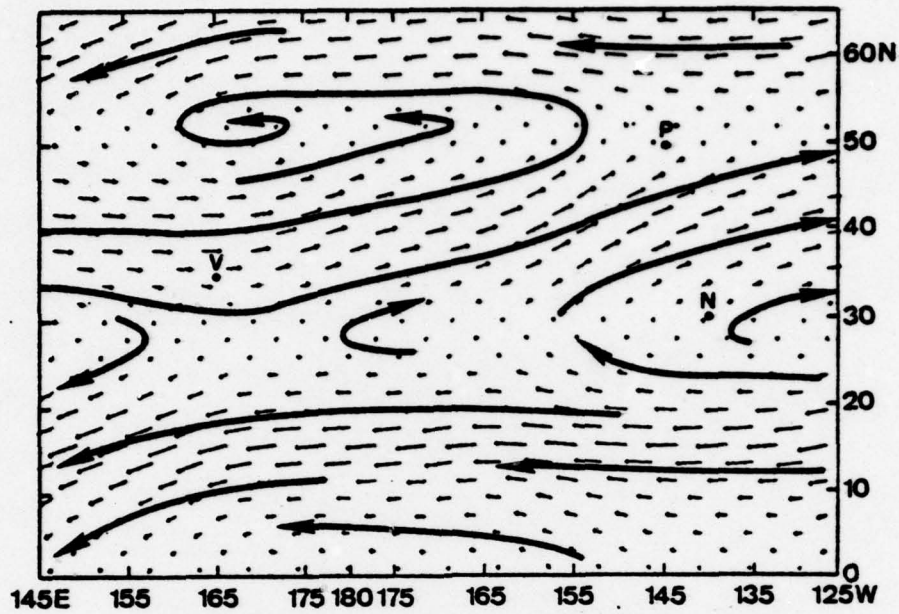(with salinity) winter (top) and summer (bottom)

Figure 27. Climatological surface wind stress
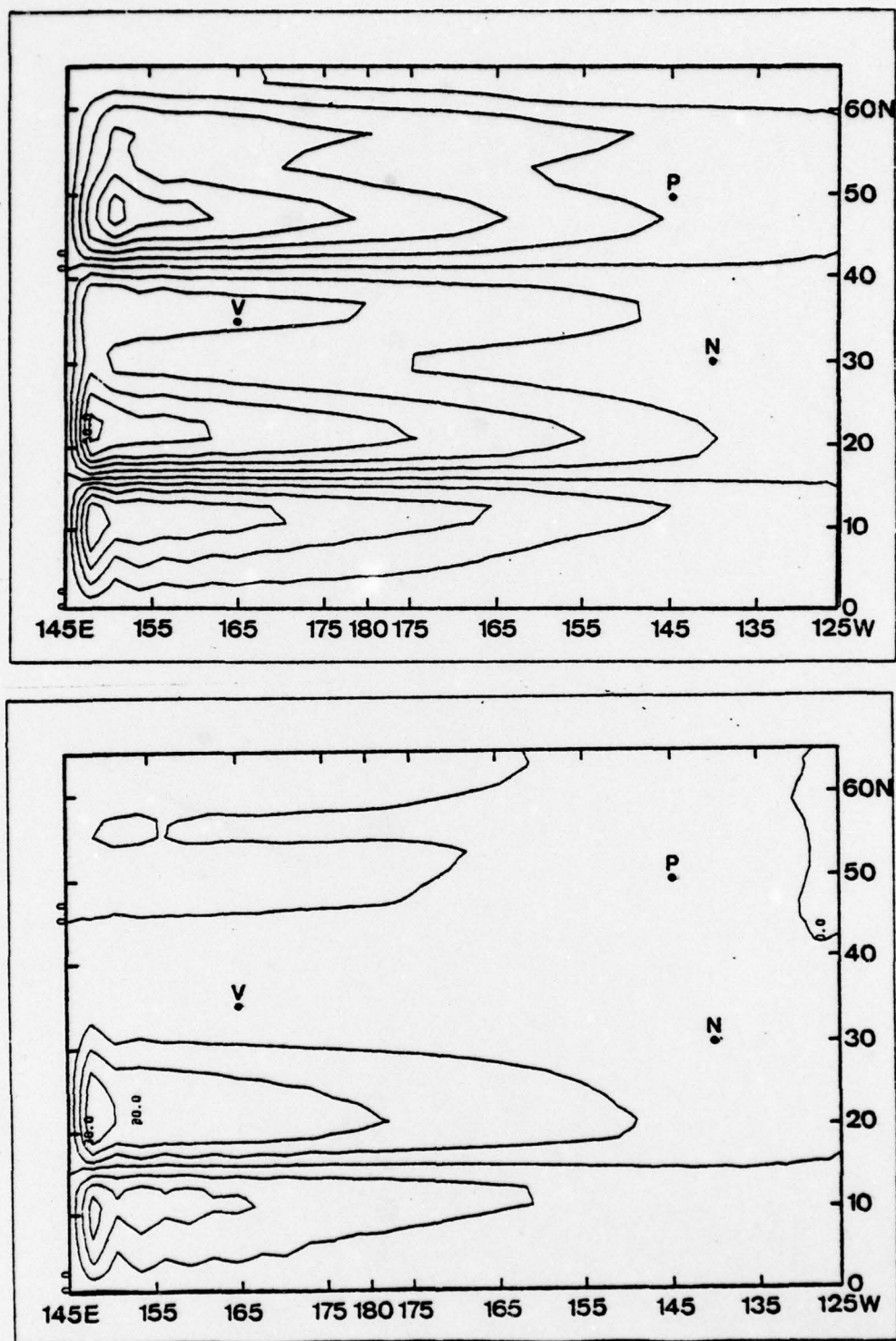patterns winter (top) and summer (bottom)

Figure 28. Transport streamfunction, winter (top)
and summer (bottom)

Figure 29. Level 3 streamlines and velocity vectors
year 248 (with salinity) summer

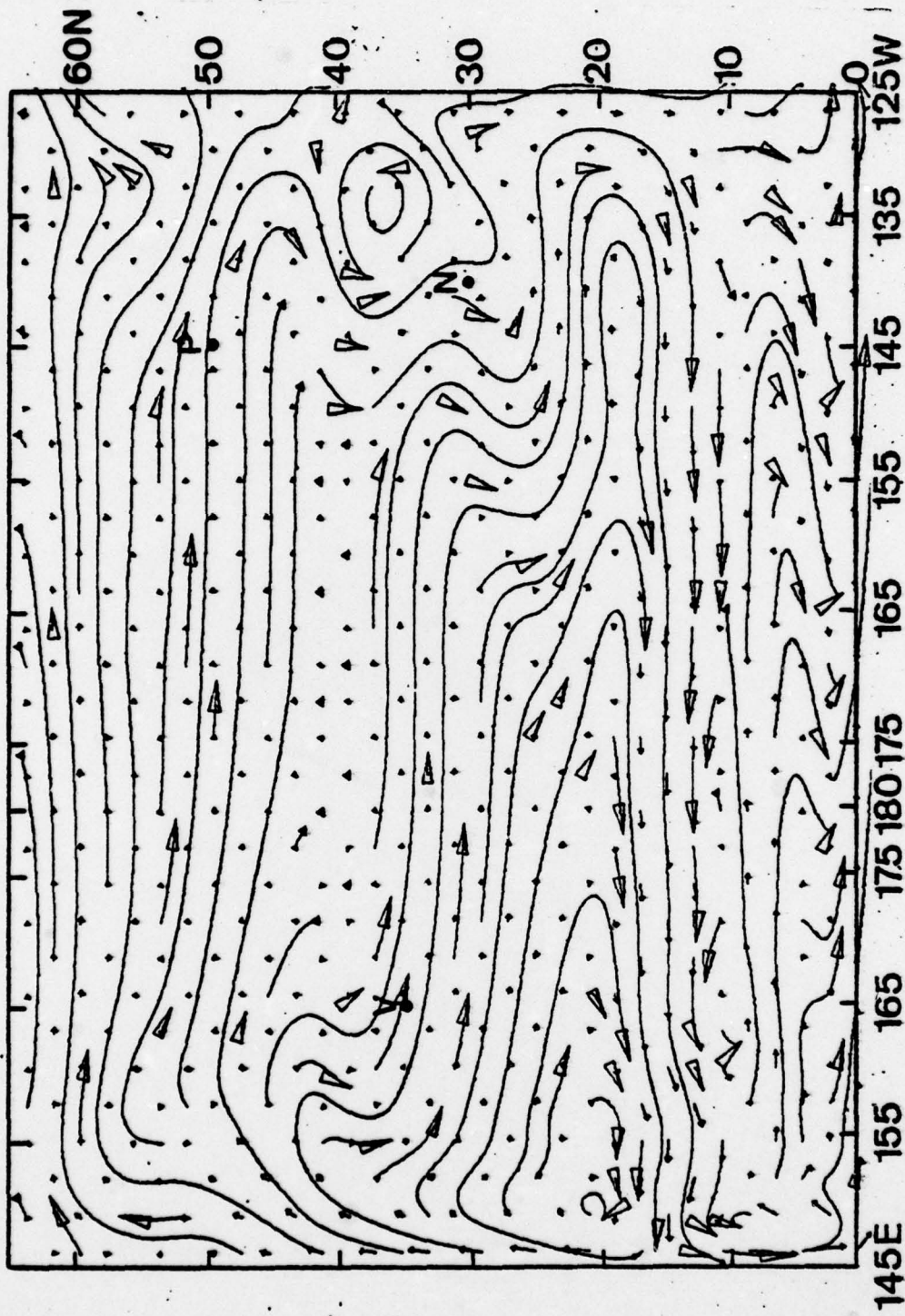Figure 30. Level 3 streamlines and velocity vectors
year 249 (with salinity) summer
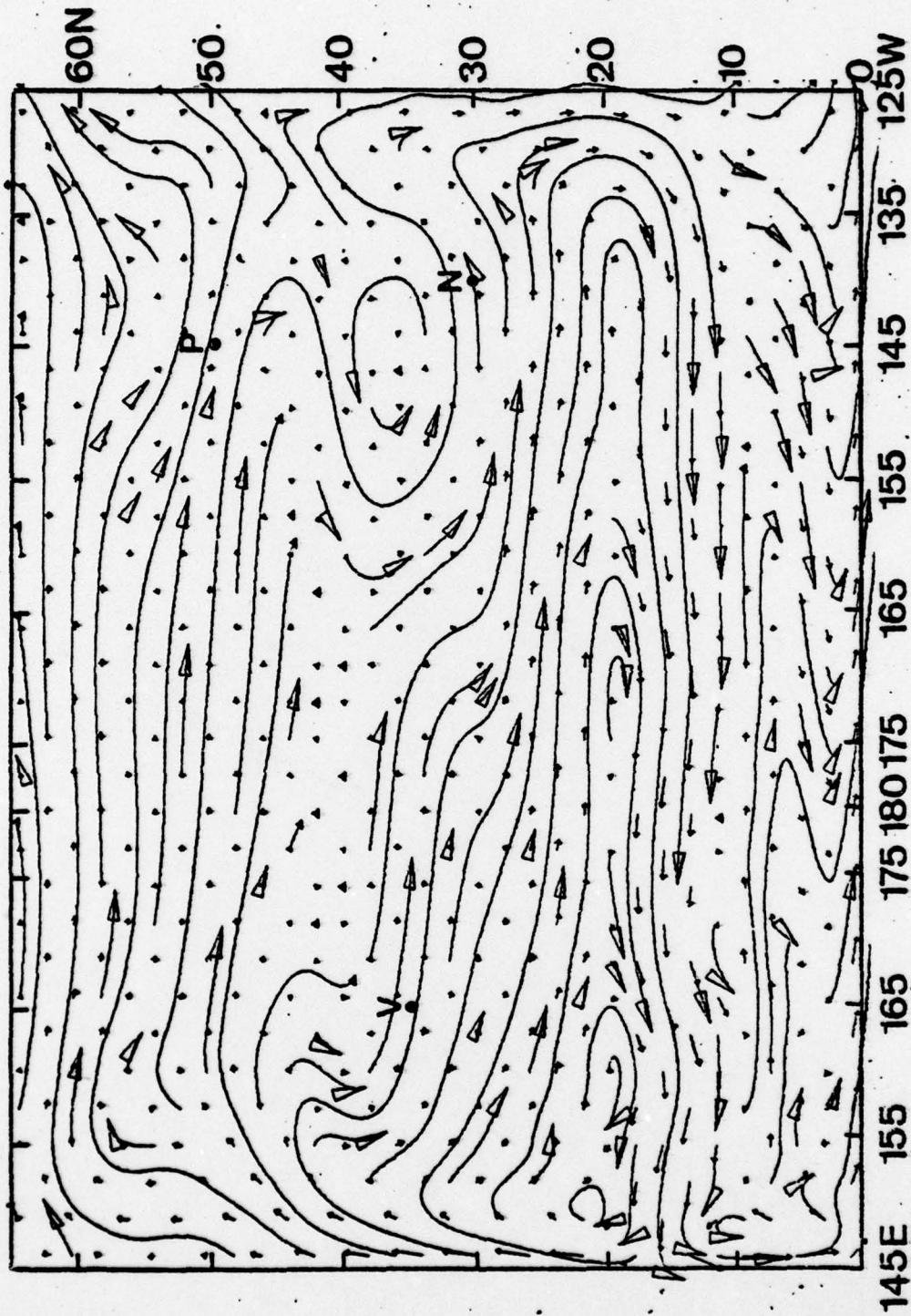
Figure 31. Level 3 streamlines and velocity vectors
year 250 (with salinity) summer
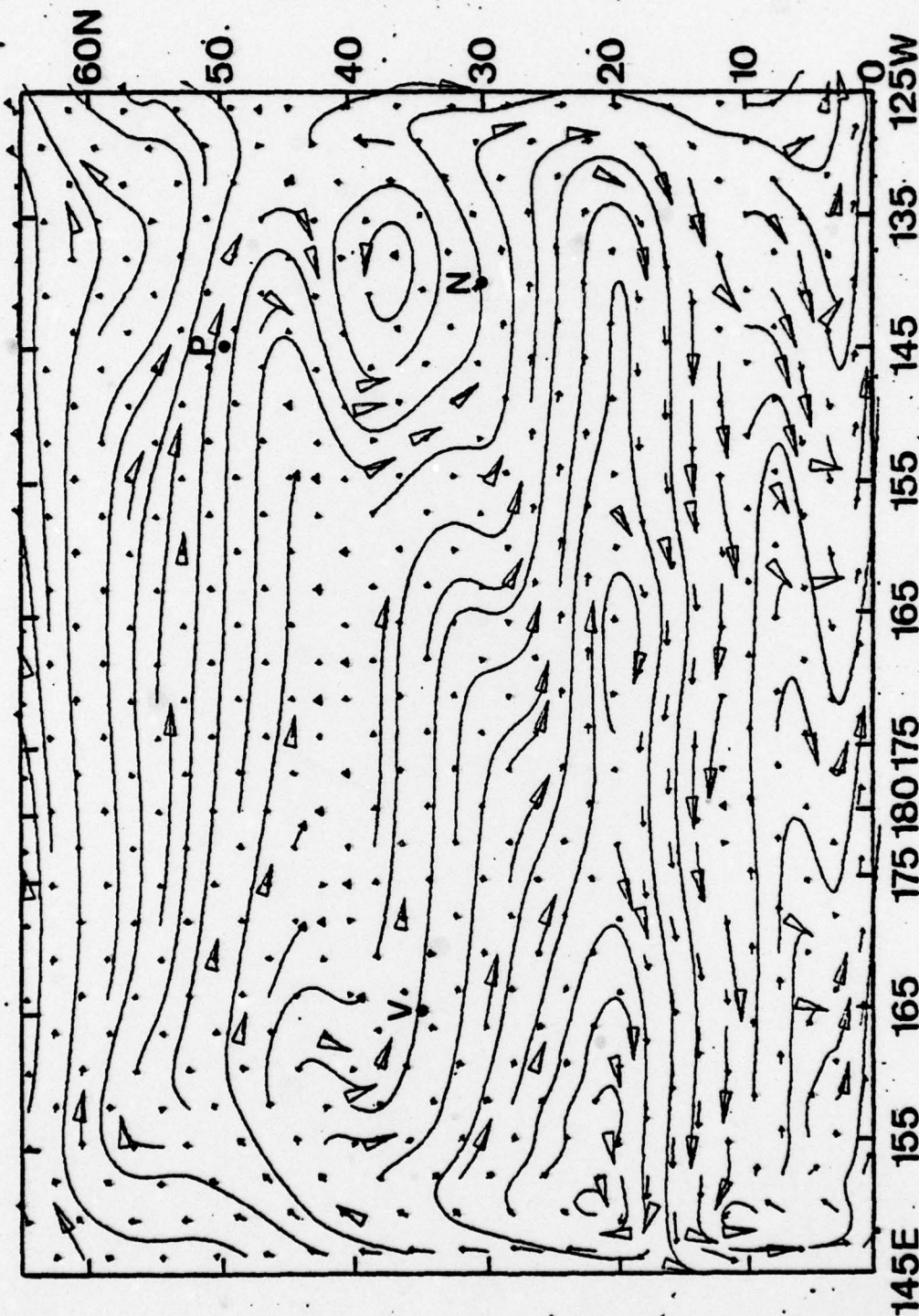
Figure 32. Level 3 streamlines and velocity vectors
year 251 (with salinity) summer

Figure 33. Level 3 temperature contours
year 248 (with salinity) summer

Figure 34. Level 3 temperature contours
year 249 (with salinity) summer
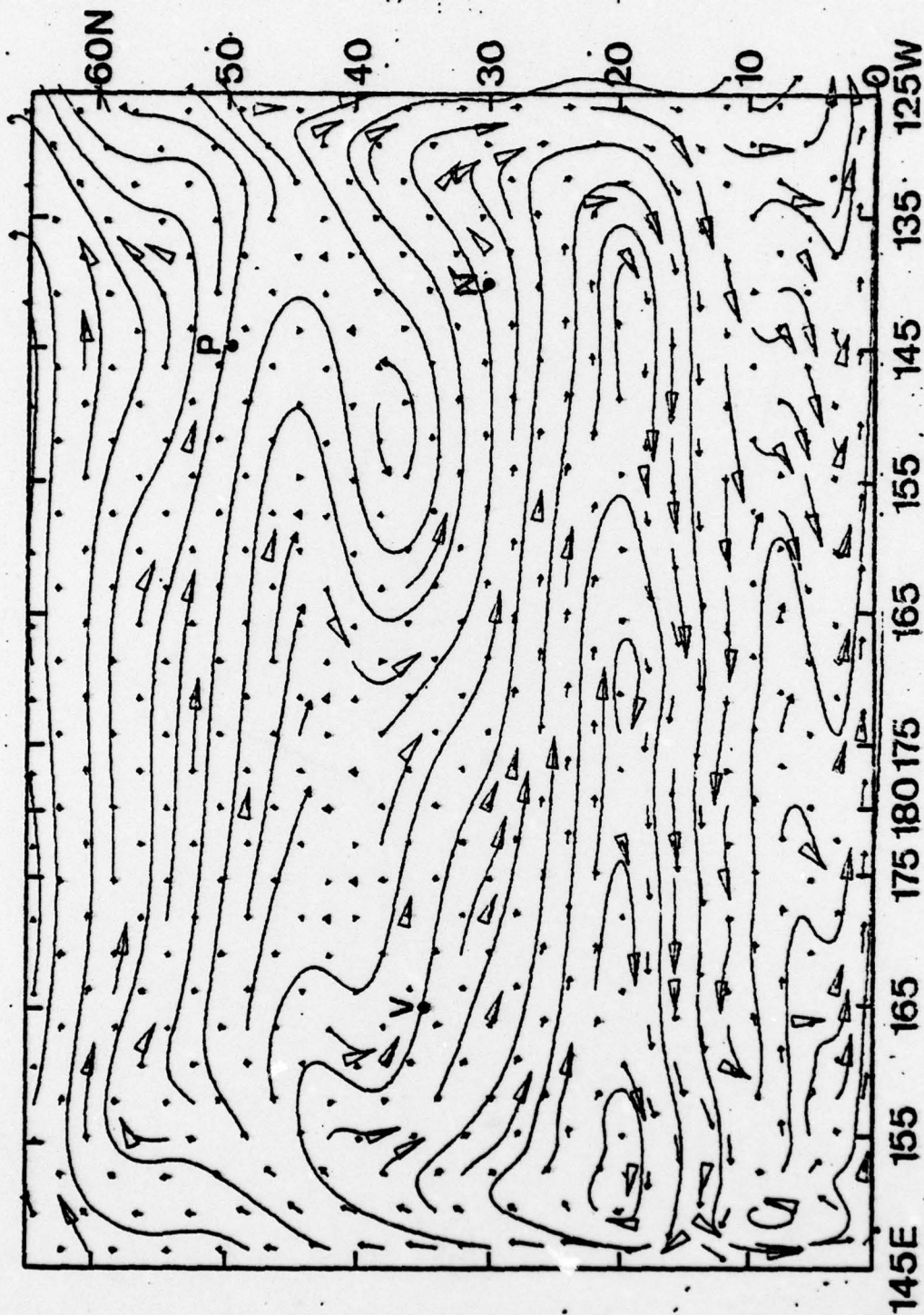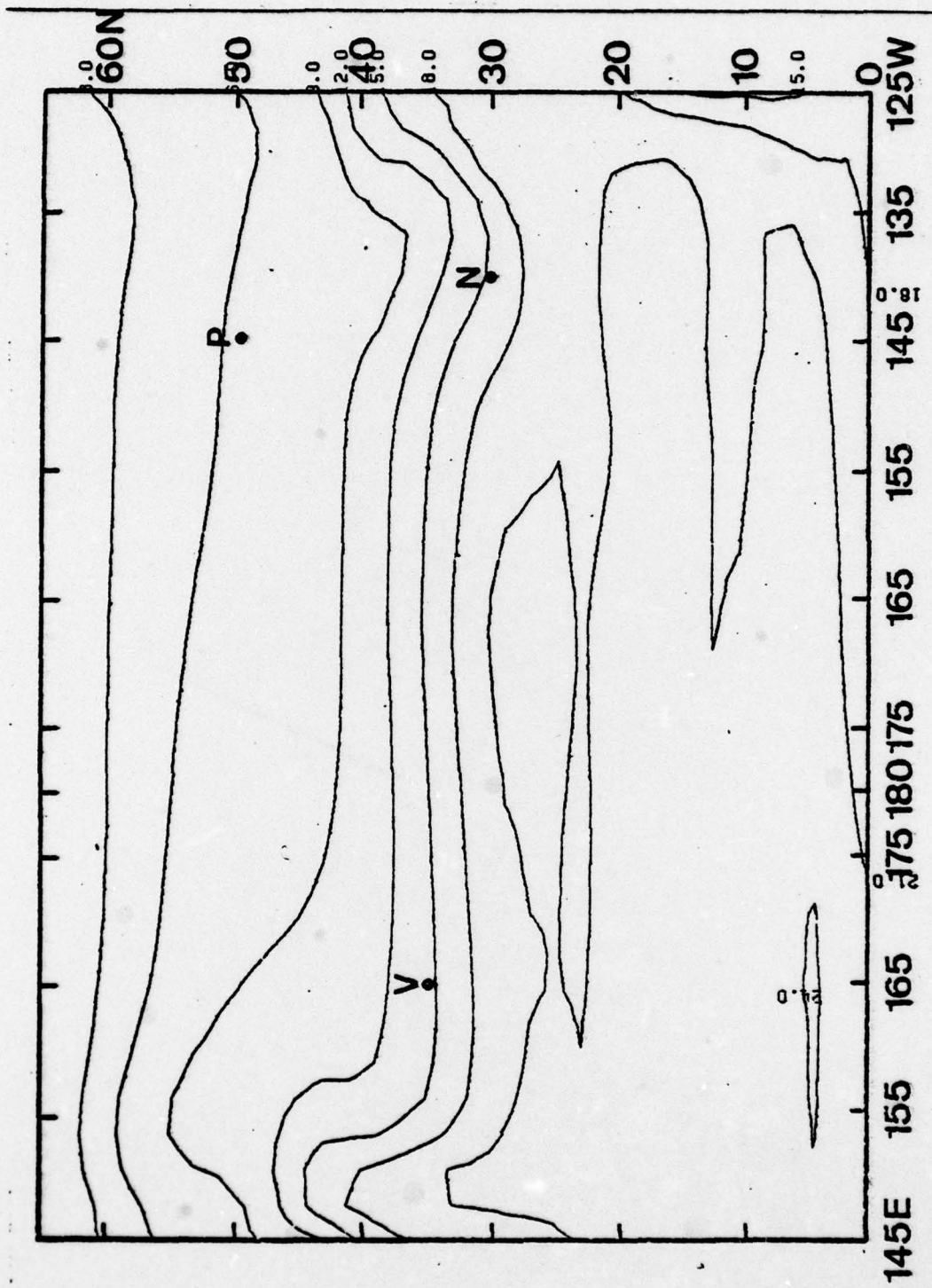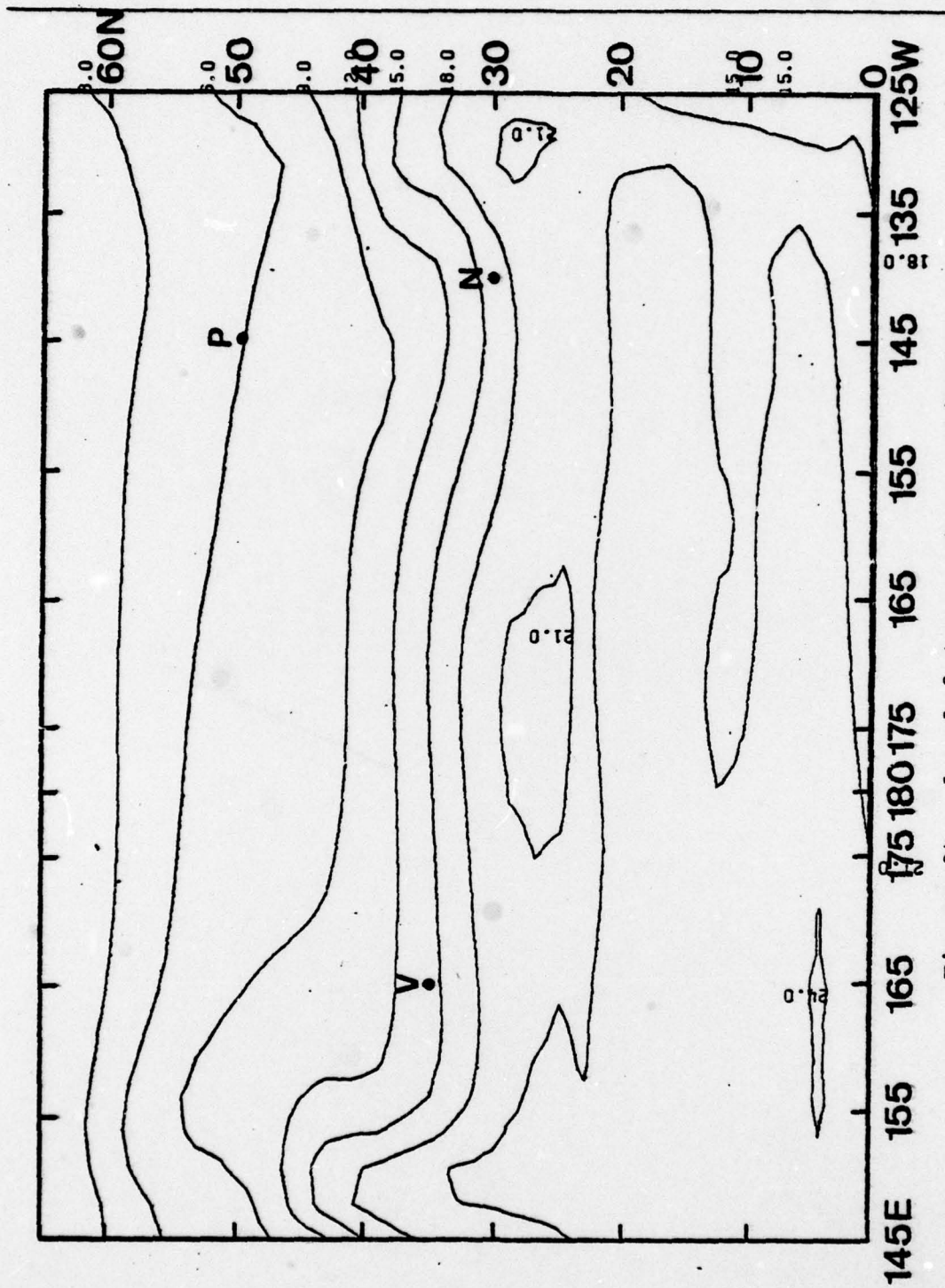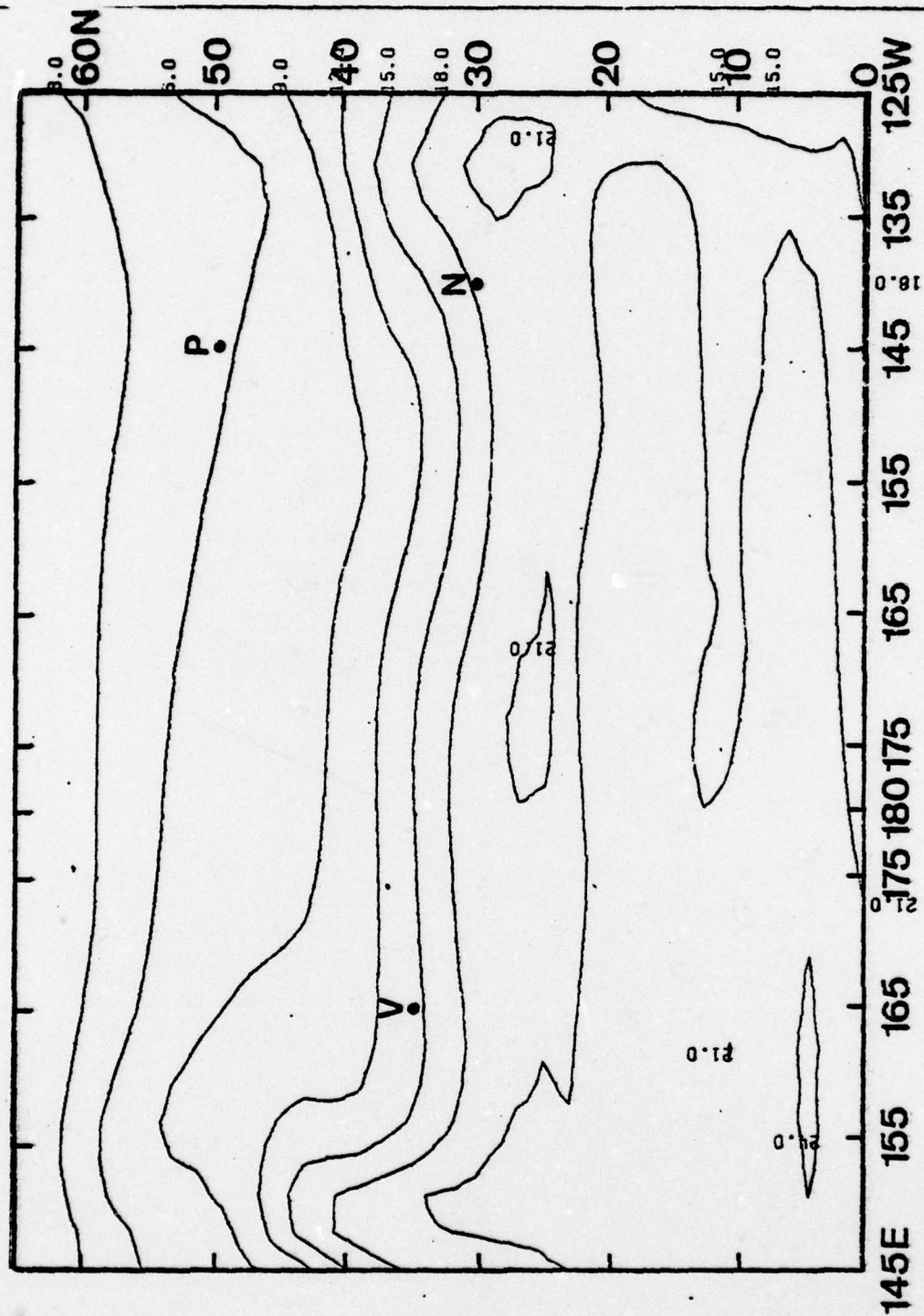
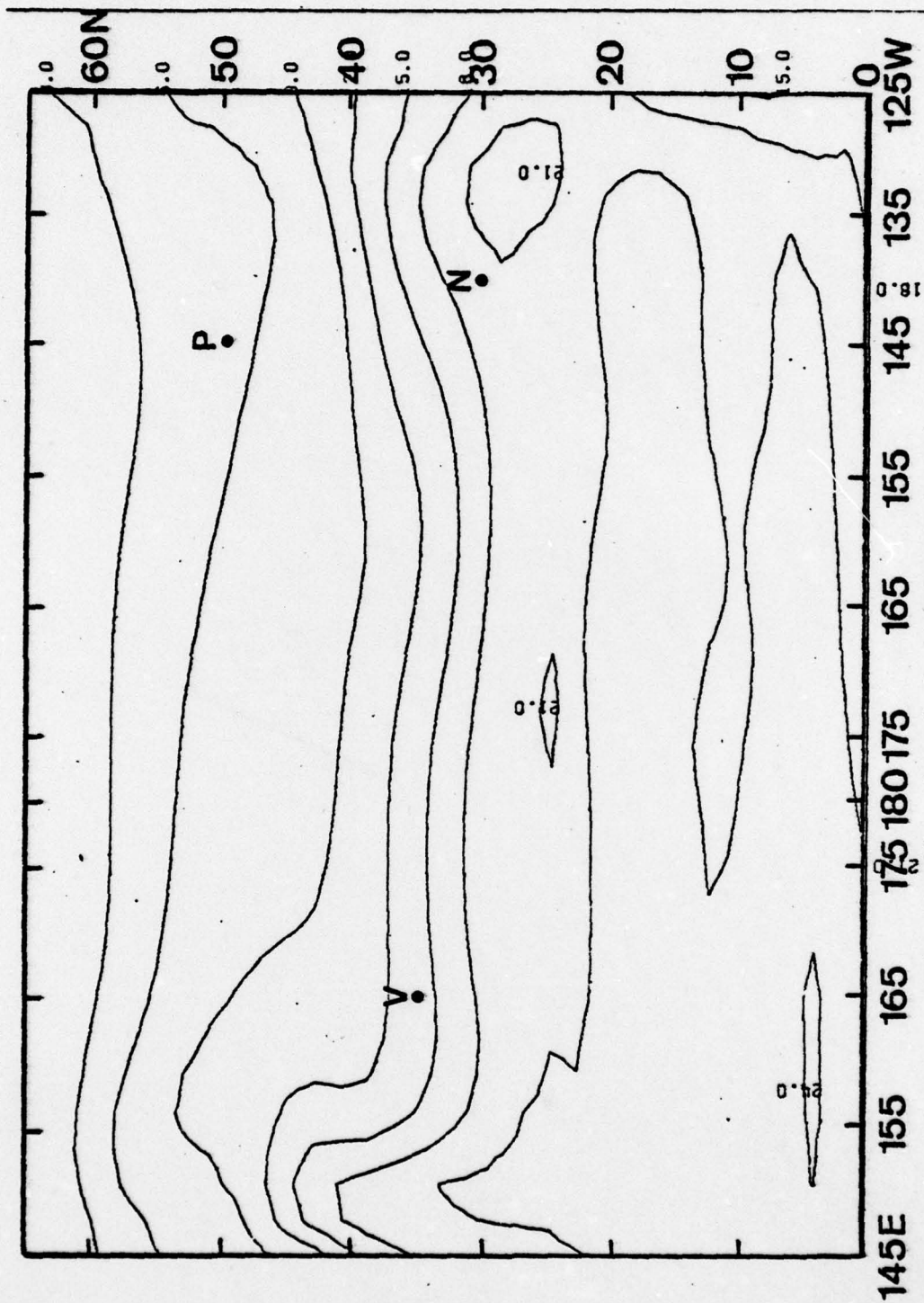Figure 35. Level 3 temperature contours
year 250 (with salinity) summer

Figure 36. Level 3 temperature contours
year 251 (with salinity) summer
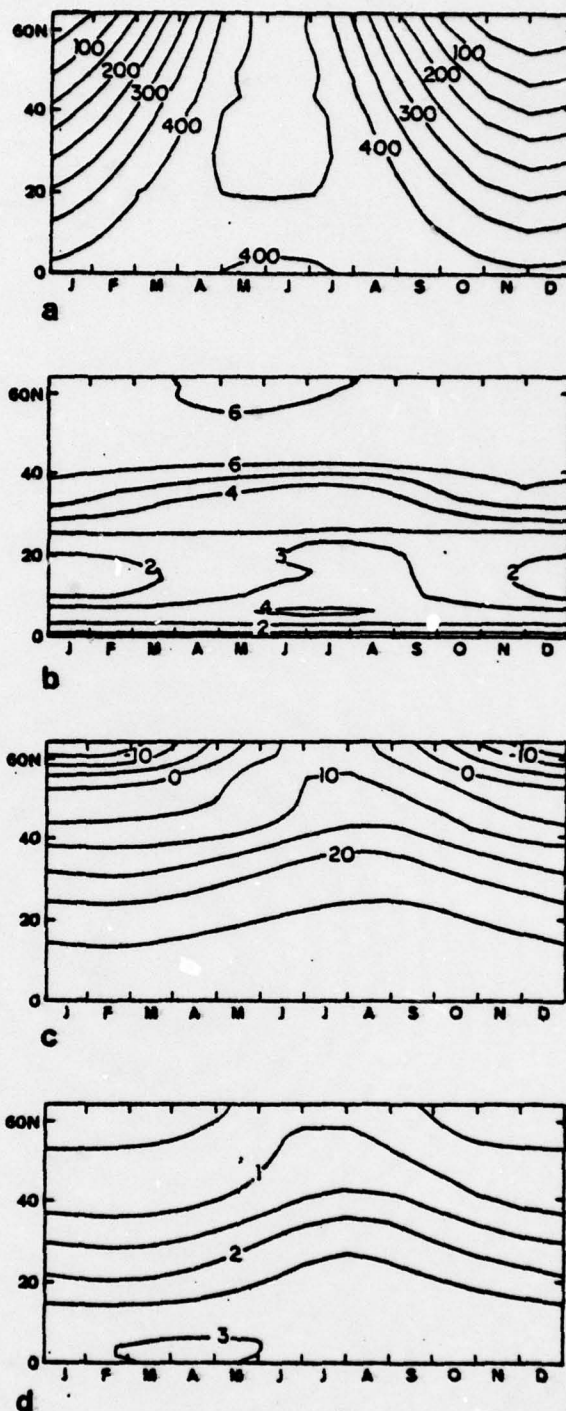
Figure 37. Climatological atmospheric quantities used in the model. (a) Solar radiation at the top of the atmosphere (Wm^{-2}); (b) fractional cloud cover (tenths); (c) surface air temperature $(°C)$; (d) surface vapor pressure (kPa)

LIST OF REFERENCES

1. Bjerknes, J., 1966: "A Possible Response of the Atmospheric Hadley Circulation to Equatorial Anomalies of Ocean Temperatures." *Tellus*, 1ö, 820-829.

2. _____, 1969: "Atmospheric Teleconnections from the Equatorial Pacific," *Mon. Wea. Rev.*, 97, 163-172.

3. _____, 1972: "Large-Scale Atmospheric Response to the 1964-65 Pacific Equatorial Warming." *J. Phy. Oceanogr.*, 2, 212-217.

4. Bryan, K., 1969: "Climate and the Ocean Circulation: III. The Ocean Model." *Mon. Wea. Rev.*, 97, 806-827.

5. _____, and M. D. Cox, 1972: "An Approximate Equation of State for Numerical Models of Ocean Circulation." *J. Phy. Oceanogr.*, 2, 510-514.

6. Friedrich, H. and S. Levitus, 1972: "An Approximation to the Equation of State for Sea Water, Suitable for Numerical Ocean Models." *J. Phy. Oceanogr.*, 2, 514-517.

7. Haney, R. L., 1974: "A Numerical Study of the Response of an Idealized Ocean to Large-Scale Surface Heat and Momentum Flux." *J. Phy. Oceanogr.*, 4, 145-167.

8. _____, and R. W. Davies, 1976: "The Role of Surface Mixing in the Seasonal Variation of the Ocean Thermal Structure." *J. Phy. Oceanogr.*, 6, 504-510.

9. _____, W. S. Shiver and K. H. Hunt, 1978: "A Dynamical-Numerical Study of the Formation and Evolution of Large-Scale Ocean Anomalies." *J. Phy. Oceanogr.*, 8, 952-969.

10. _____, and J. Wright, 1975: "The Relationship between the Grid Size and the Coefficient of Nonlinear Lateral Eddy Viscosity in Numerical Ocean Circulation Models." *J. Computational Physics*, 19, 257-266.

11. Hunt, K. H., 1975: *The Prediction of Sea-Surface Temperature Anomalies Using a 10-Level Primitive Equation Model*. M.S. Thesis, Department of Meteorology, Naval Postgraduate School, Monterey, California, 83 pp.

12. Manabe, S., 1969: "Climate and the Ocean Circulation: II. The Atmospheric Circulation and the Effects of Heat Transfer by Ocean Currents." *Mon. Wea. Rev.*, 97, 775-805.

13. Namias, J., 1959: "Recent Seasonal Interactions between North Pacific Water and the Overlying Atmospheric Circulation." J. Geophy. Res., 64, 631-646.

14. _____, 1969: "Seasonal Interactions between the North Pacific Ocean and the Atmosphere during the 1960's." Mon. Wea. Rev., 97, 173-192.

15. _____, 1972: "Experiments in Objectively Predicting some Atmospheric and Oceanic Variables for the Winter of 1971-72." J. Appl. Meteor., 11, 1164-1174.

16. Scripps Institution of Oceanography, University of California, 1960: Oceanic Observations of the Pacific: 1955, The NORPAC Data. Berkeley and Los Angeles, University of California Press, 532 pp.

17. _____, 1963a: Oceanic Observations of the Pacific: 1951. Berkeley and Los Angeles, University of California Press, 598 pp.

18. _____, 1963b: Oceanic Observations of the Pacific: 1956. Berkeley and Los Angeles, University of California Press, 458 pp.

19. _____, 1965a: Oceanic Observations of the Pacific: 1952. Berkeley and Los Angeles, University of California Press, 617 pp.

20. _____, 1965b: Oceanic Observations of the Pacific: 1954. Berkeley and Los Angeles, University of California Press, 426 pp.

21. _____, 1965c: Oceanic Observations of the Pacific: 1957. Berkeley and Los Angeles, University of California Press, 707 pp.

22. _____, 1965d: Oceanic Observations of the Pacific: 1959. Berkeley and Los Angeles, University of California Press, 901 pp.

23. Shiver, W. S., 1977: Dynamical Numerical Prediction of Large-Scale Thermal Anomalies in the North Pacific Ocean. M. S. Thesis, Department of Meteorology, Naval Postgraduate School, Monterey, California, 47 pp.

24. Sverdrup, H. U., M. W. Johnson and R. H. Fleming, 1942: The Oceans, their Physics, Chemistry and General Biology. Prentice Hall, New York, 1087 pp.

25. Reid, J. L., Jr., 1965: Intermediate Waters of the Pacific Ocean. Johns Hopkins Press, Baltimore, 85 pp.

26. Riley, J. P. and G. Skirrow, 1975: Chemical Oceanography, Vol. I. Academic Press, London, 606 pp.

27. Rowntree, P. R., 1972: "The Influence of Tropical East Pacific Ocean Temperatures on the Atmosphere." Quart. J. Roy. Meteor. Soc., 98, 290-321.

28. Wetherald, R. T. and S. Manabe, 1972: "Response of the Joint Ocean-Atmosphere Model to the Seasonal Variation of the Solar Radiation." Mon. Wea. Rev., 100, 42-59.

INITIAL DISTRIBUTION LIST

No. Copies

1. Defense Documentation Center   2
   Cameron Station
   Alexandria, Virginia 22314

2. Library, Code 0142   2
   Naval Postgraduate School
   Monterey, California 93940

3. Dr. R. L. Haney, Code 63Hy   3
   Department of Meteorology
   Naval Postgraduate School
   Monterey, California 93940

4. Lieutenant K. E. Barbor   2
   604 Ryder Cup
   Virginia Beach, Virginia 23462

5. Meteorology Department Library, Code 63Lib   1
   Naval Postgraduate School
   Monterey, California 93940

6. Dr. G. J. Haltiner, Code 63Ha   1
   Chairman, Department of Meteorology
   Naval Postgraduate School
   Monterey, California 93940

7. Dr. G. H. Jung, Code 68Jg   1
   Department of Oceanography
   Naval Postgraduate School
   Monterey, California 93940

8. Dr. William J. Emery   1
   Institute of Oceanography
   University of British Columbia
   Vancouver, B.C. CANADA, V6T 1W5

9. Prof. Gunnar I. Roden   1
   Dept. of Oceanography
   University of Washington
   Seattle, Washington 98195